Heterojunctions for Photocatalysis

Eric Wei-Guang Diau（刁維光）
Department of Applied Chemistry
Institute of Molecular Science
National Yang-Min Chiao-Tung University (NYCU)
Hsinchu, Taiwan

Solar Energy

- Sun is renewable, clean energy resource, available across the globe.
- Solar radiation energy density on the surface of earth is about 1 kW/m^2

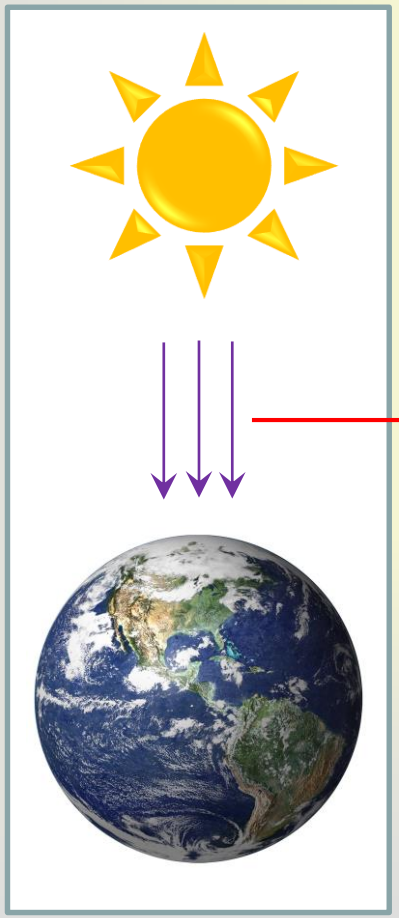

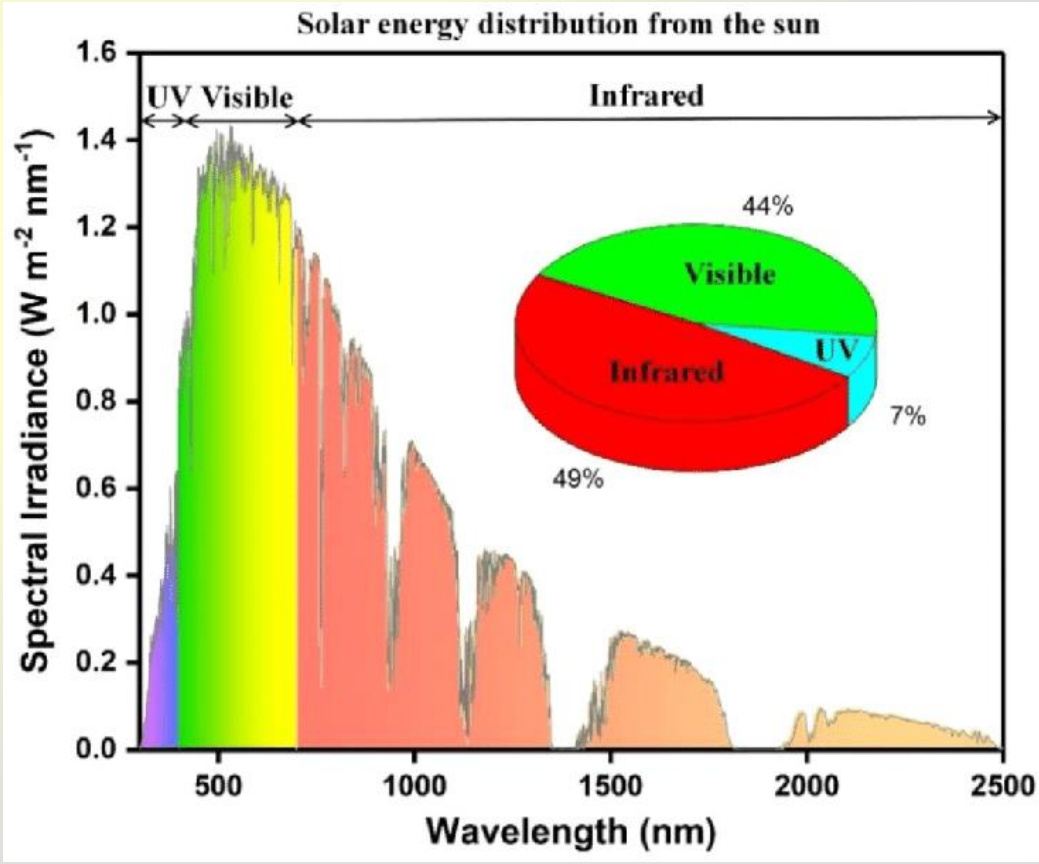

Renew. Sust. Energ. Rev., 152 (2021) 111615

Principle of Photocatalysis

Photocatalysts harvest solar energy and convert it to chemical energy.

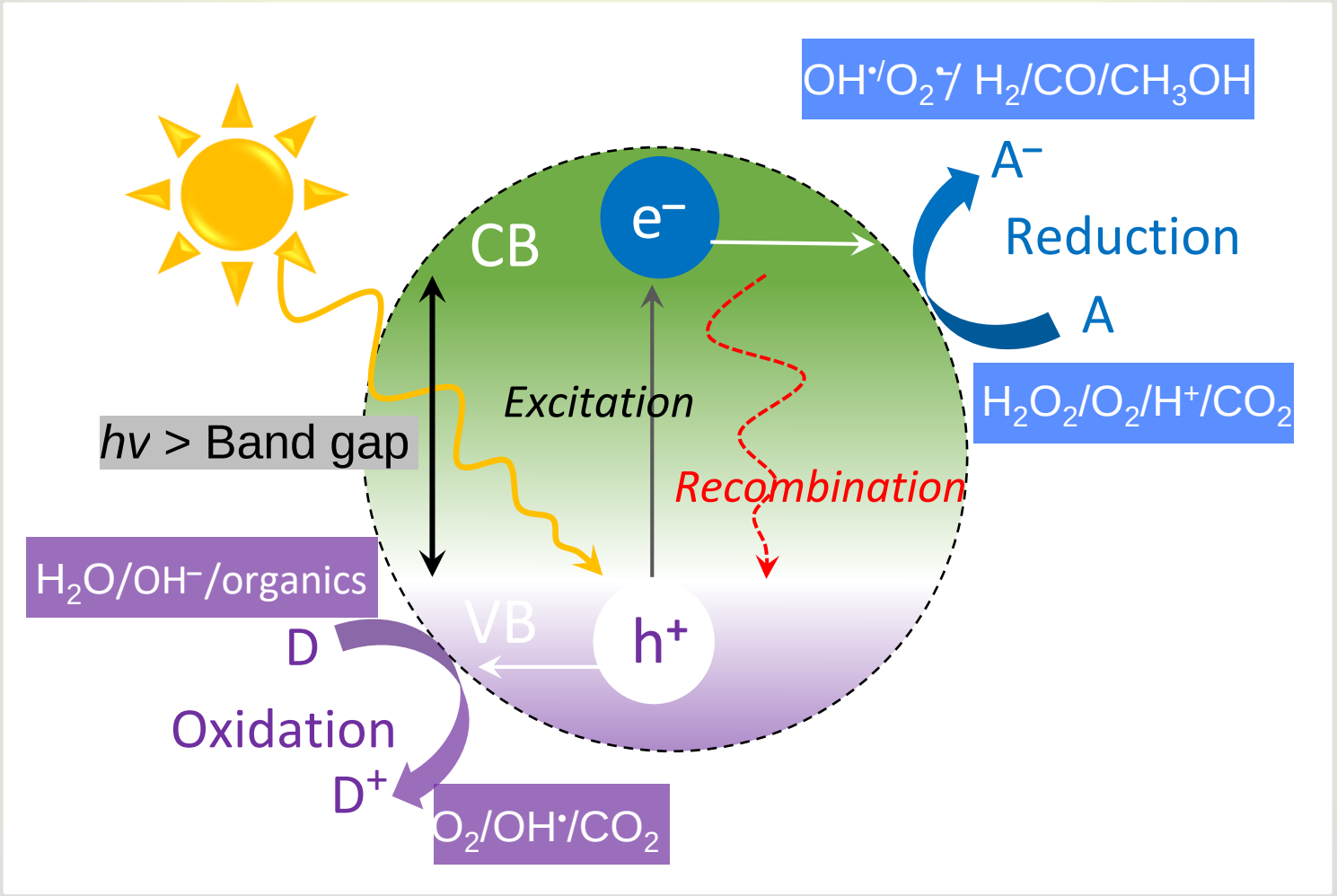

From Single Photocatalyst to Heterojunction

Ideal Photocatalyst

(i) Photogenerated charges with long lifetimes

(ii) An appropriate band gap

(iii) Full range of sunlight utilization

(iv) Low cost

(v) High efficiency

(vi) High stability

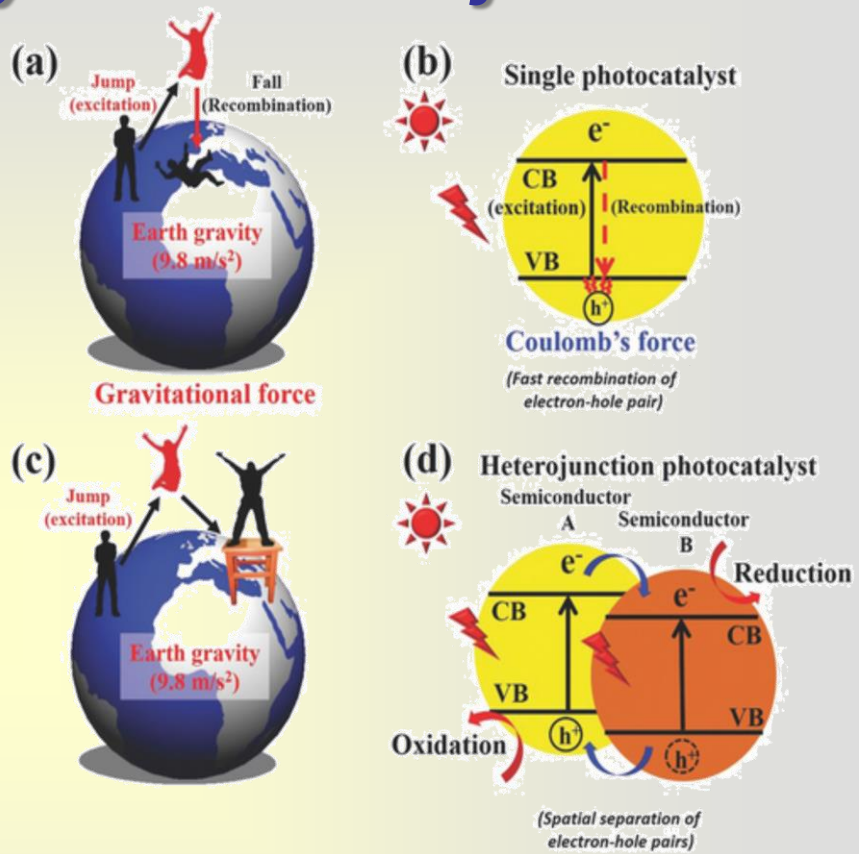

a) the effect of gravitational force on a man who jumps off the ground, b) electron–hole recombination on a single photocatalyst, c) use of a stool to keep a man off the ground, and d) electron–hole separation on a heterojunction photocatalyst.

Single Photocatalyst

*** Norrow Band Gap**

*** Low Carrier Recombination**

*** Broad sunlight absorption**

*** Strong redox ability**

Adv. Mater. 2017, 29, 1601694.

Fabrication of 2D-based and Perovskite Heterojunctions

Top-Down Fabrication of 2D-based Heterojunctions

Exfoliated from the bulk crystal by:

- Chemical reactions

- Mechanical effect such as liquid-phase exfoliation

- Mechanical cleavage

- Etching method

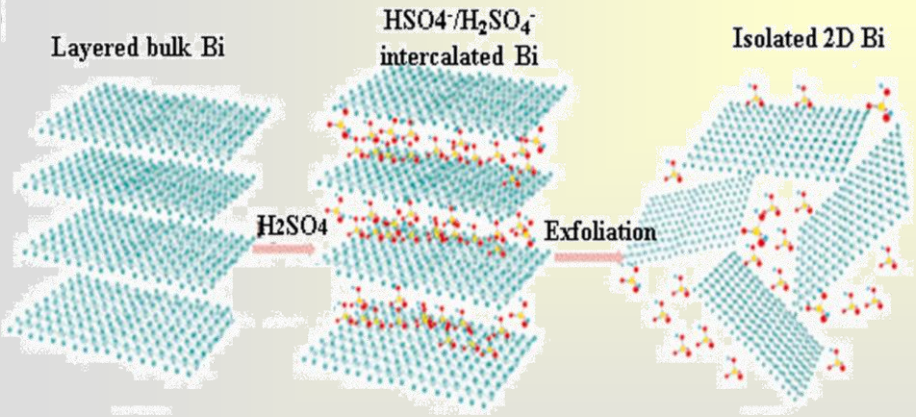

H_2SO_4-assisted liquid exfoliation of bulk Bi into Bi nanosheets.

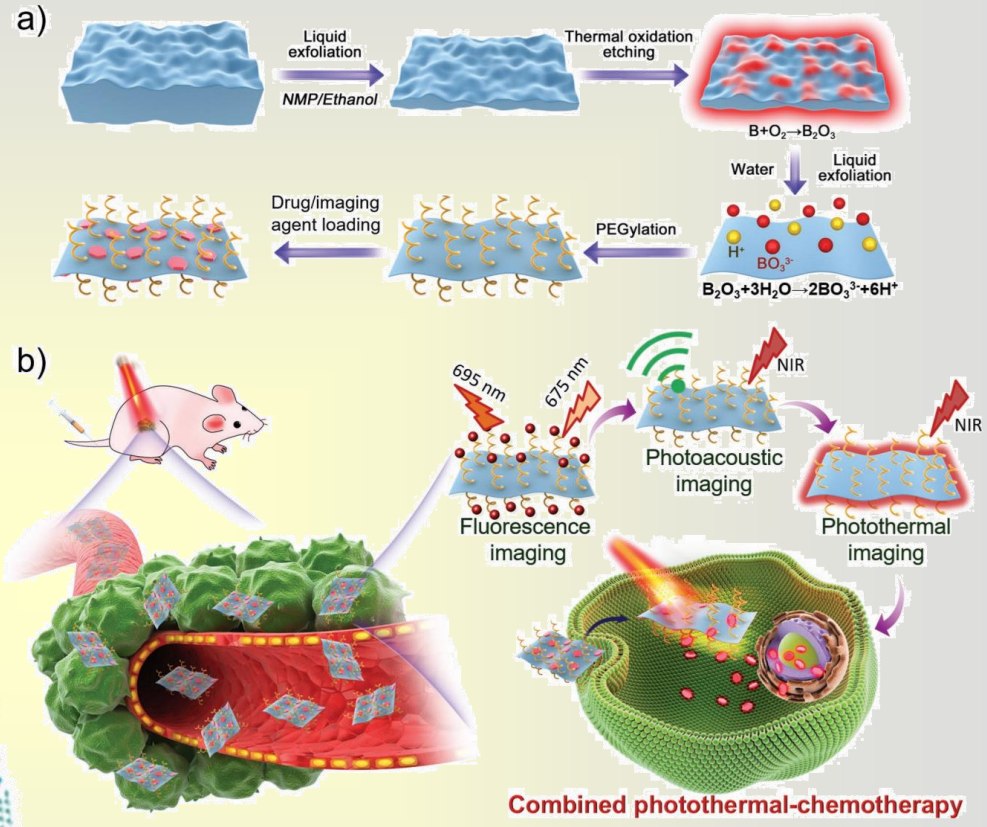

Ultrathin boron nanosheets (B NSs) are prepared by coupling thermal oxidation etching and liquid exfoliation technologies.

- Journal of Hazardous Materials 405, 2021, 124179
- Adv. Mater. 30 (36), 2018, 1803031
- Nanoscale, 10, 2018, 21106–21115.

Bottom-up Fabrication of 2D-based Heterojunctions

Growing the nanosheets directly from atoms, ions, or molecules:

- **Chemical Vapor Deposition (CVD)**
- **Physical Vapor Deposition (PVD)**
- **Thermal Deposition**
- **Plasma Assisted Deposition**
- **Wet-chemical reactions such as Hydrothermal and Solvothermal**
- **Hot Injection**
- **Ligand assisted reprecipitation**

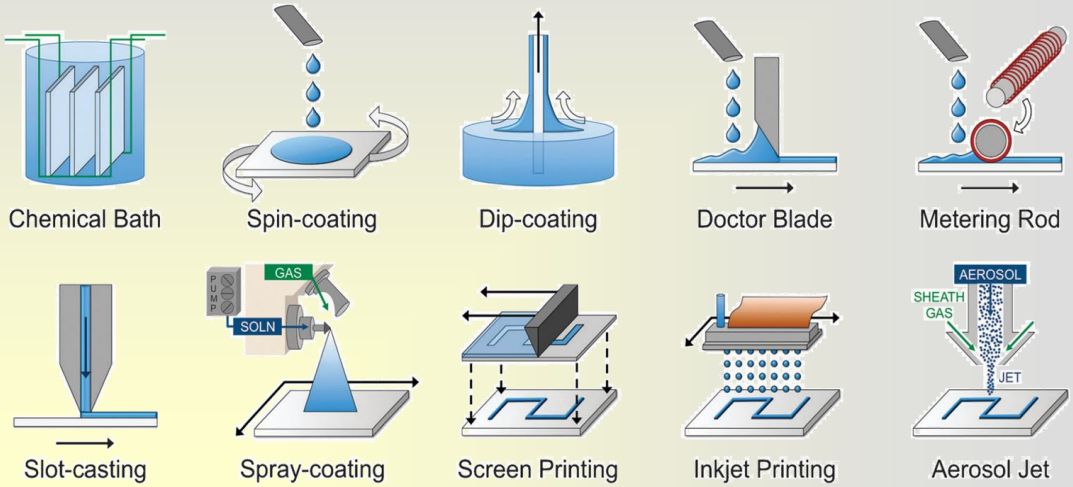

Depiction of various solution deposition method.

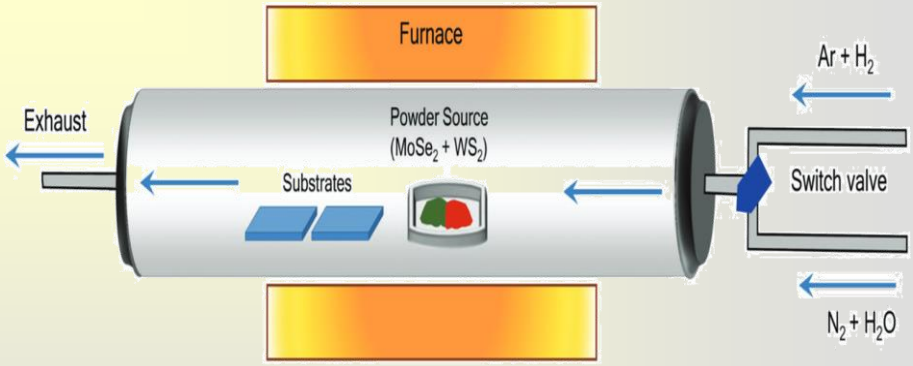

Schematics of the CVD growth process.

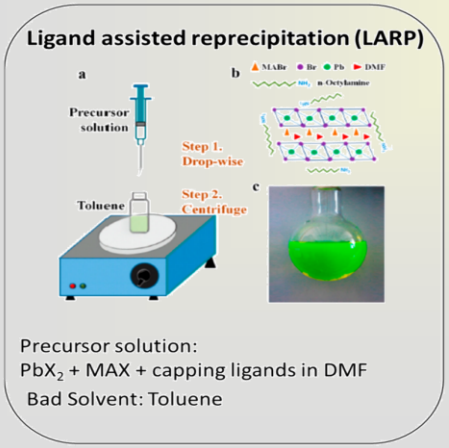

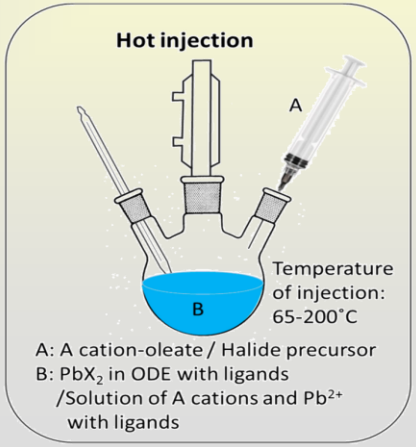

Small, 18, 2022, 2106600.
Crystals, 8, 2018, 182.
Chem. Soc. Rev., 40, 2011, 5406–5441

Engineering of Heterojunctions

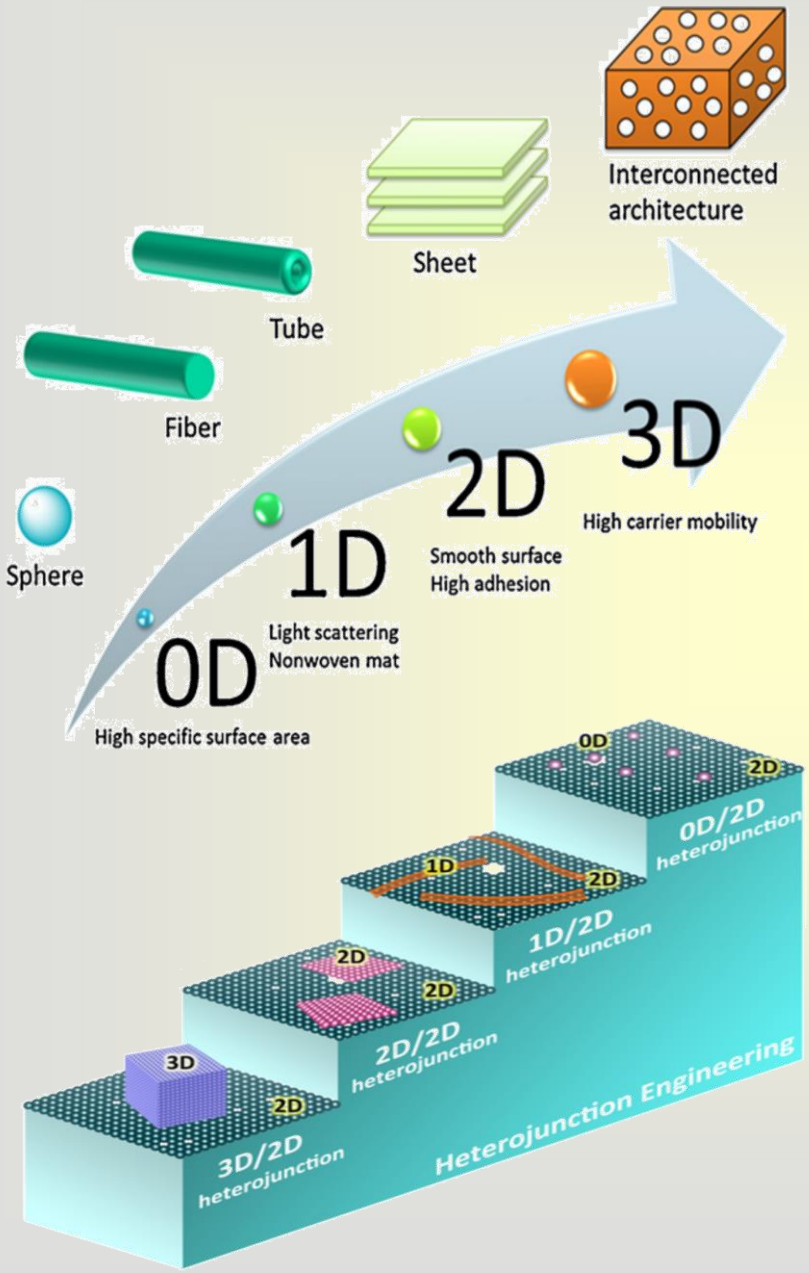

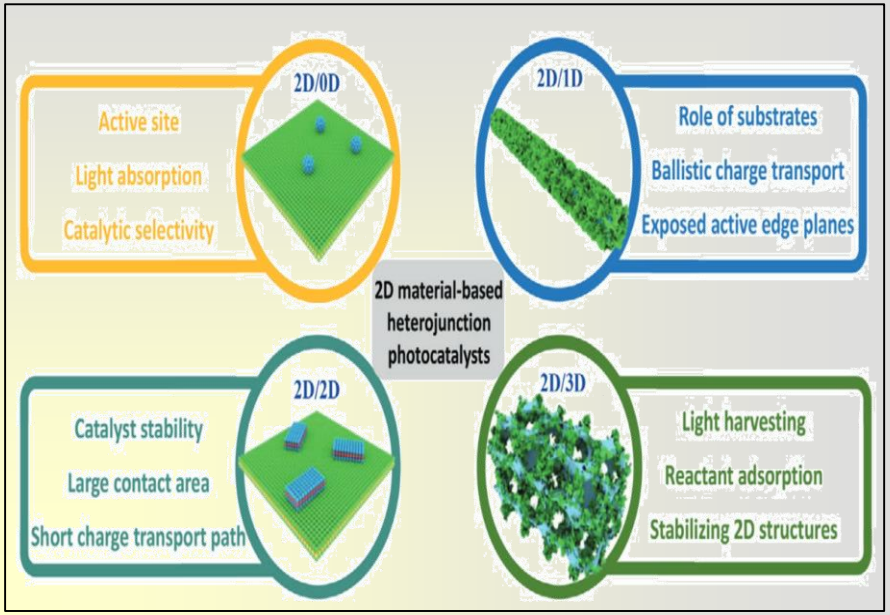

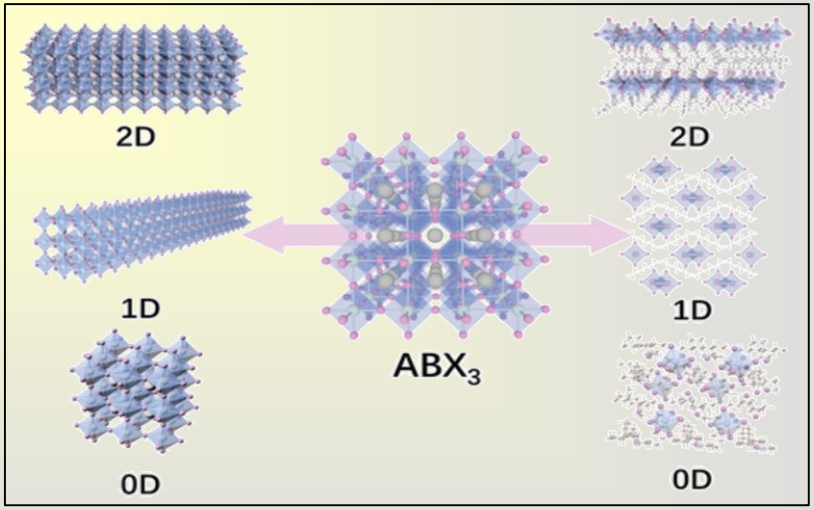

- Sol. RRL, 4, 2020, 20001322000132.
- Adv. Sustainable Syst., 4, 2020, 2000130.
- Adv Optical Mater, 10, 2022, 2102661.

Categorizations of Perovskite Heterojunctions

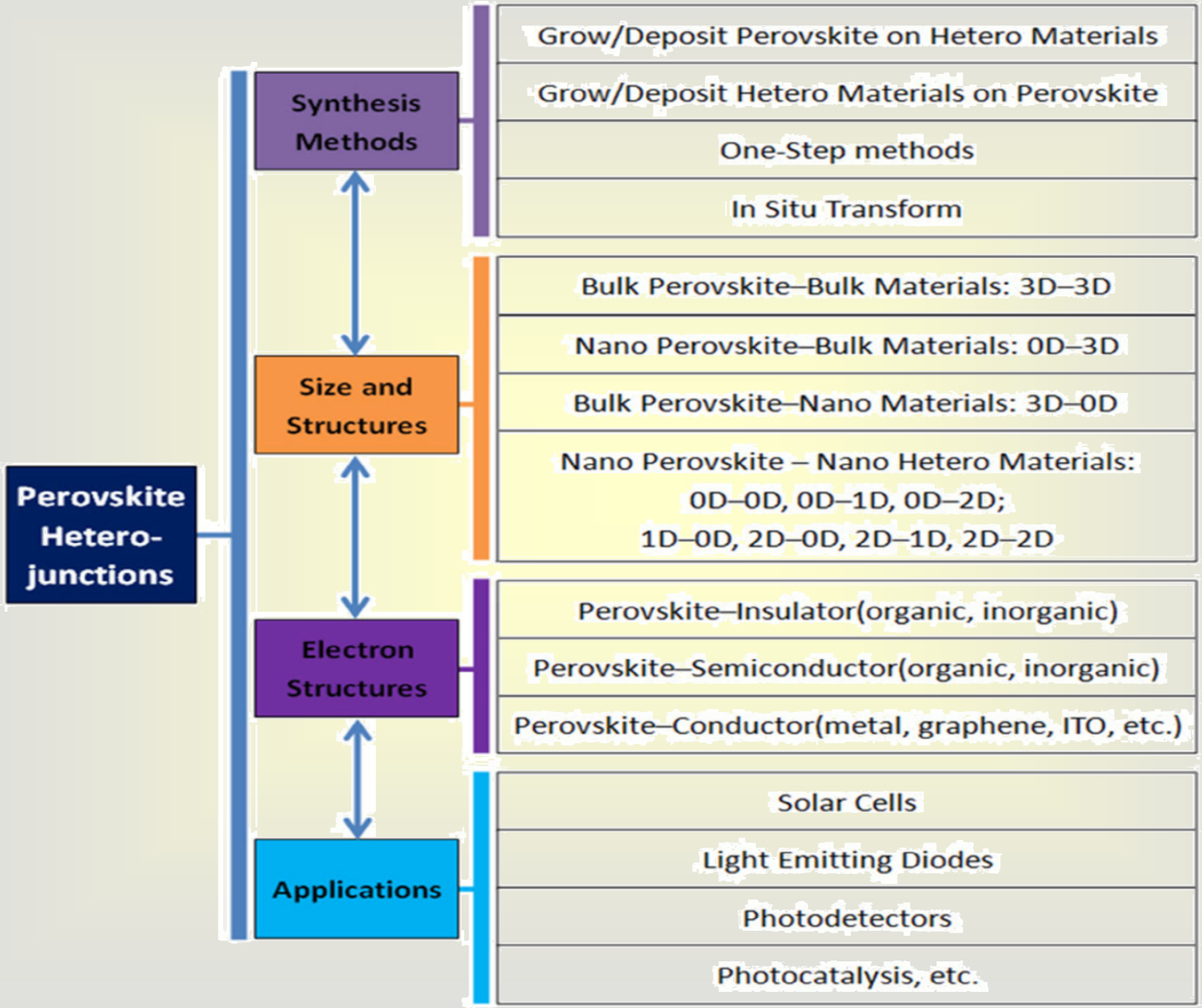

Small Struct. 1(1), 2020, 2000009

Synthetic Methods of Perovskite Materials

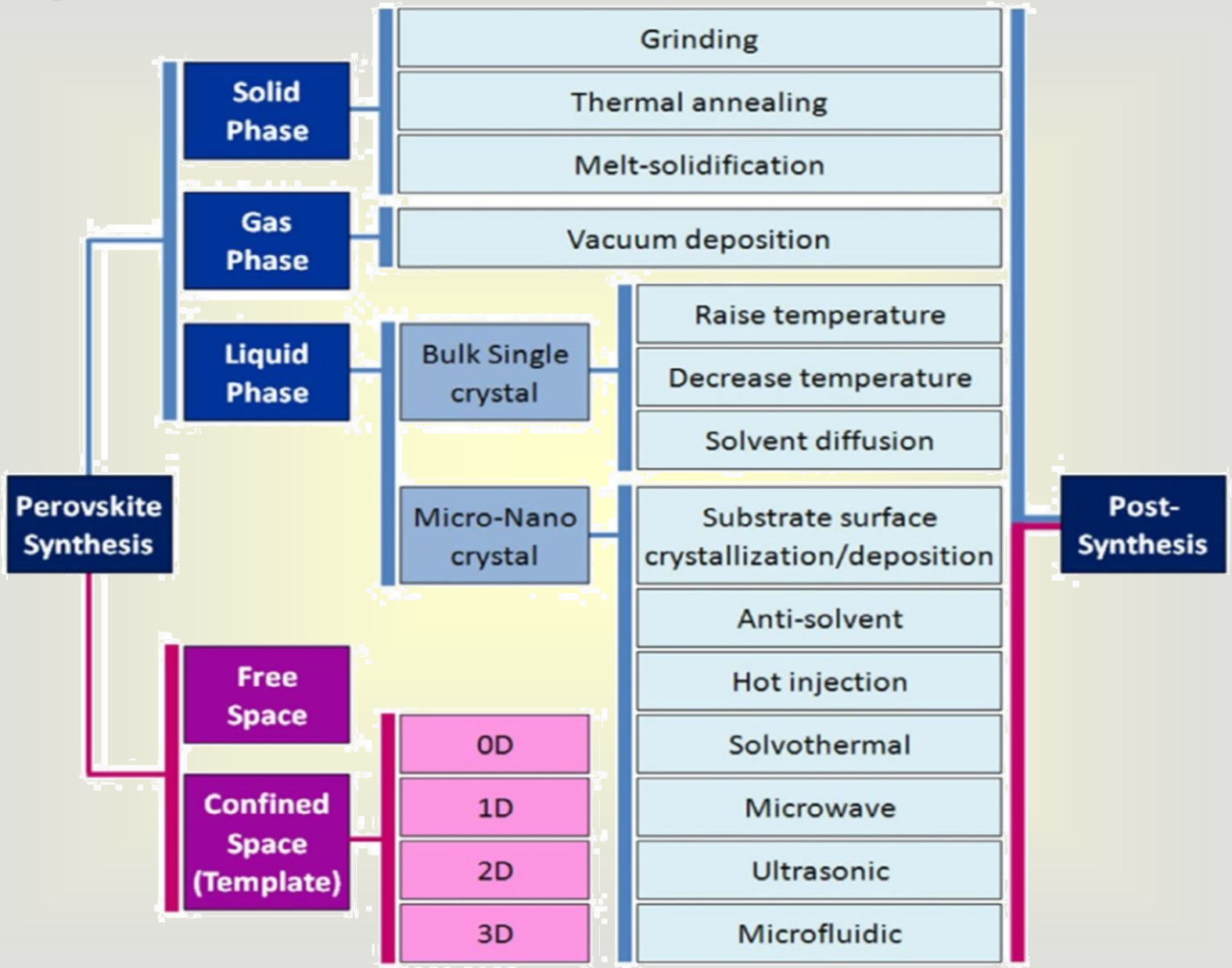

Small Struct. 1(1), 2020, 2000009

Classification of Photocatalysts with Varied Types of Heterojunctions

Heterojunction Photocatalysts

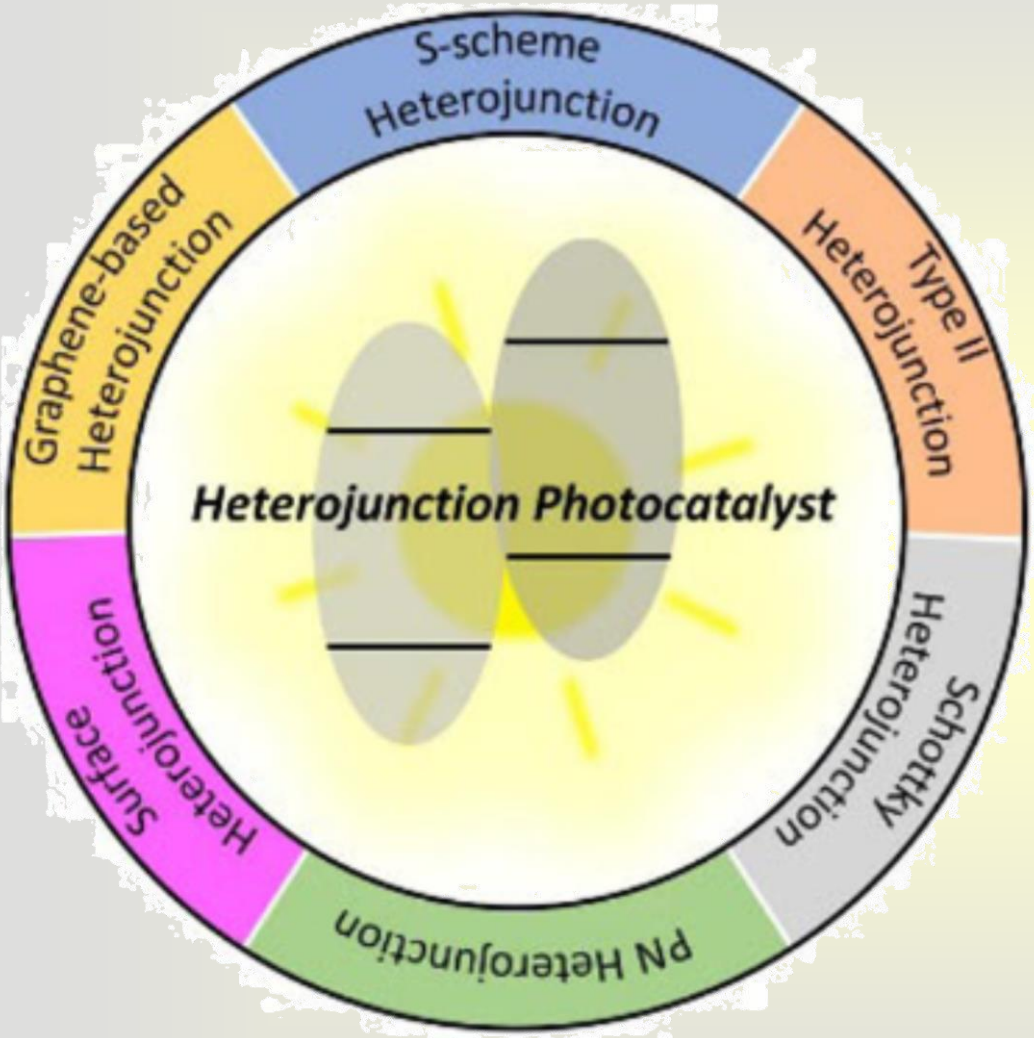

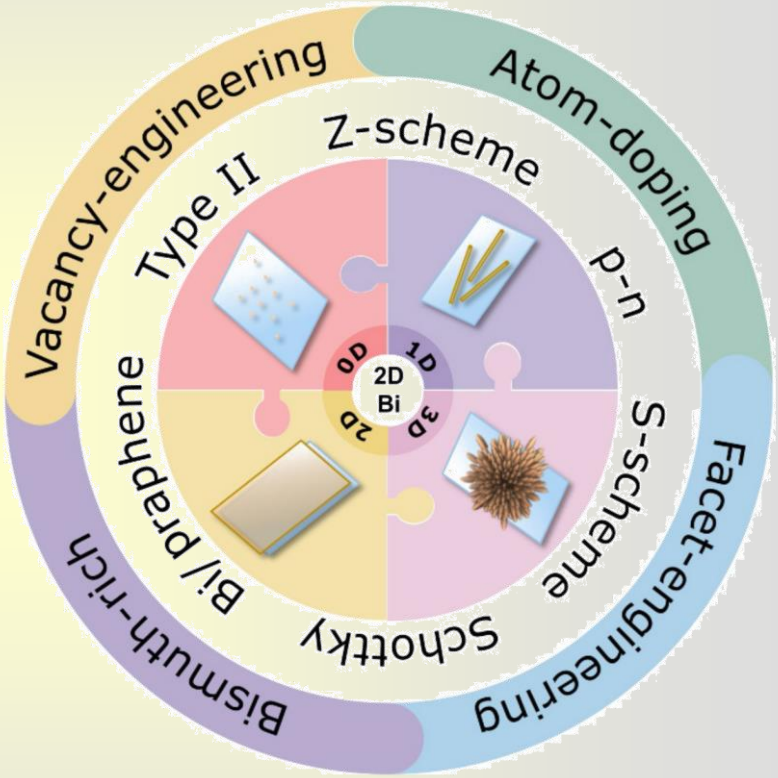

Chinese Journal of Catalysis 42 (2021) 710–730

Nano Research, 2022, 261

Semiconductor–Semiconductor Heterojunctions

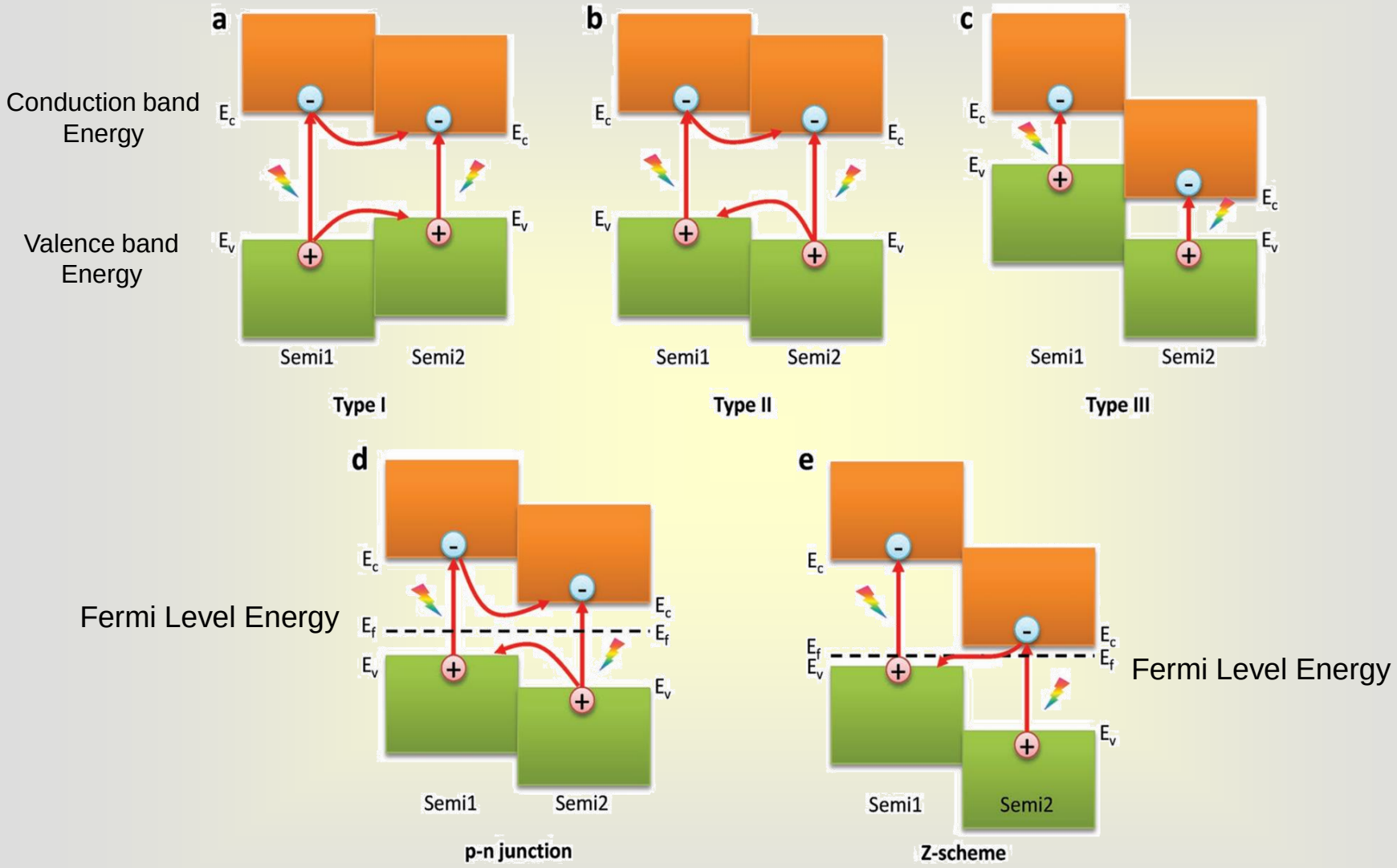

Band diagrams illustrating the various possibilities in the formation of heterojunctions between semiconductor1 (semi1) and semiconductor 2 (semi2): a) Type I, b) Type II, c) Type III, d) p–n junction, and e) Z-scheme

Adv. Funct. Mater. 30(15) 2020, 1908984

What is Fermi level?

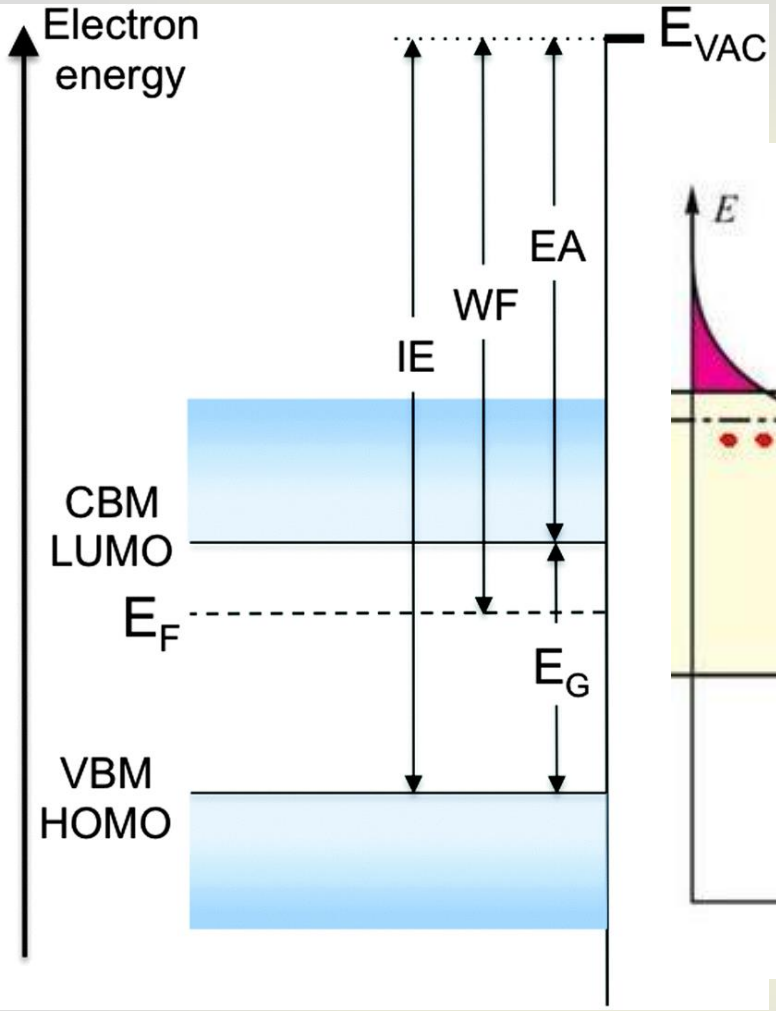

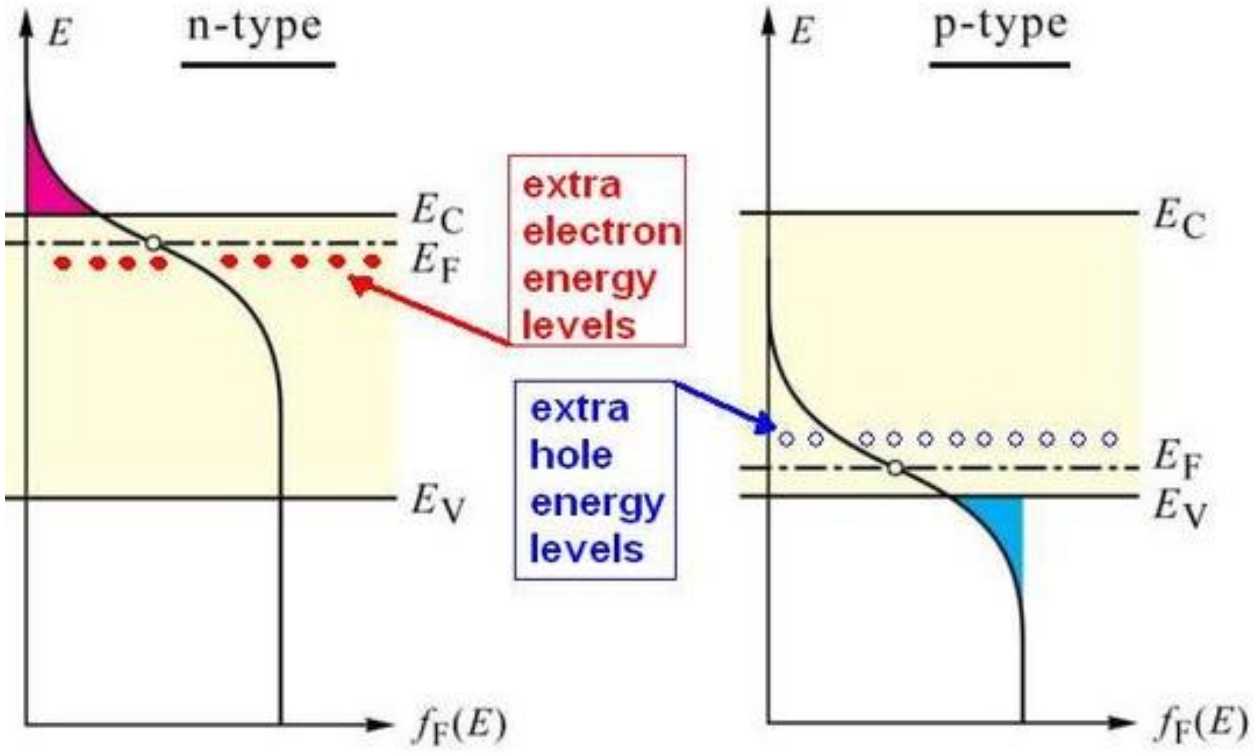

The highest energy level that an electron can occupy at the absolute zero temperature is known as the Fermi Level. The Fermi level lies between the valence band and conduction band because at absolute zero temperature the electrons are all in the lowest energy state. Due to the lack of sufficient energy at 0 Kelvin, the Fermi level can be considered as the sea of fermions (or electrons) above which no electrons exist. The Fermi level changes as the solids are warmed and as electrons are added to or

Schottky Junctions for a Semiconduction and a Metal

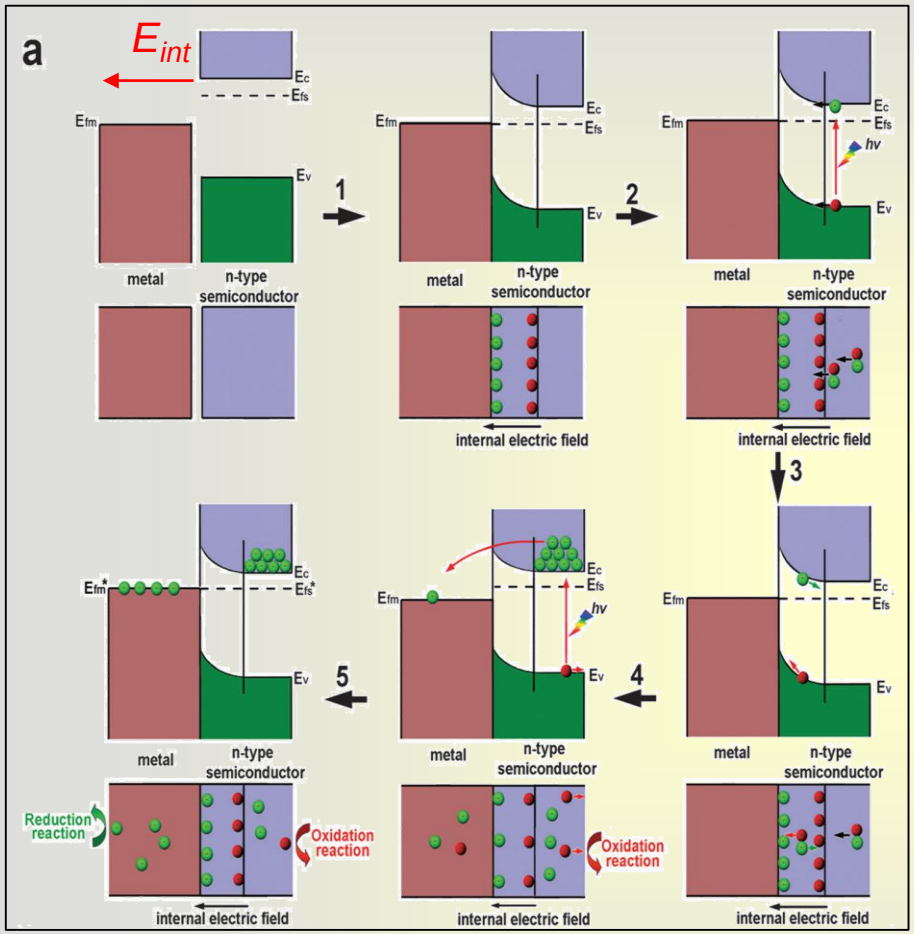

(a) Schematic illustrating processes of charge separation and transfer driven by the Schottky junction between a metal and an n-type semiconductor;

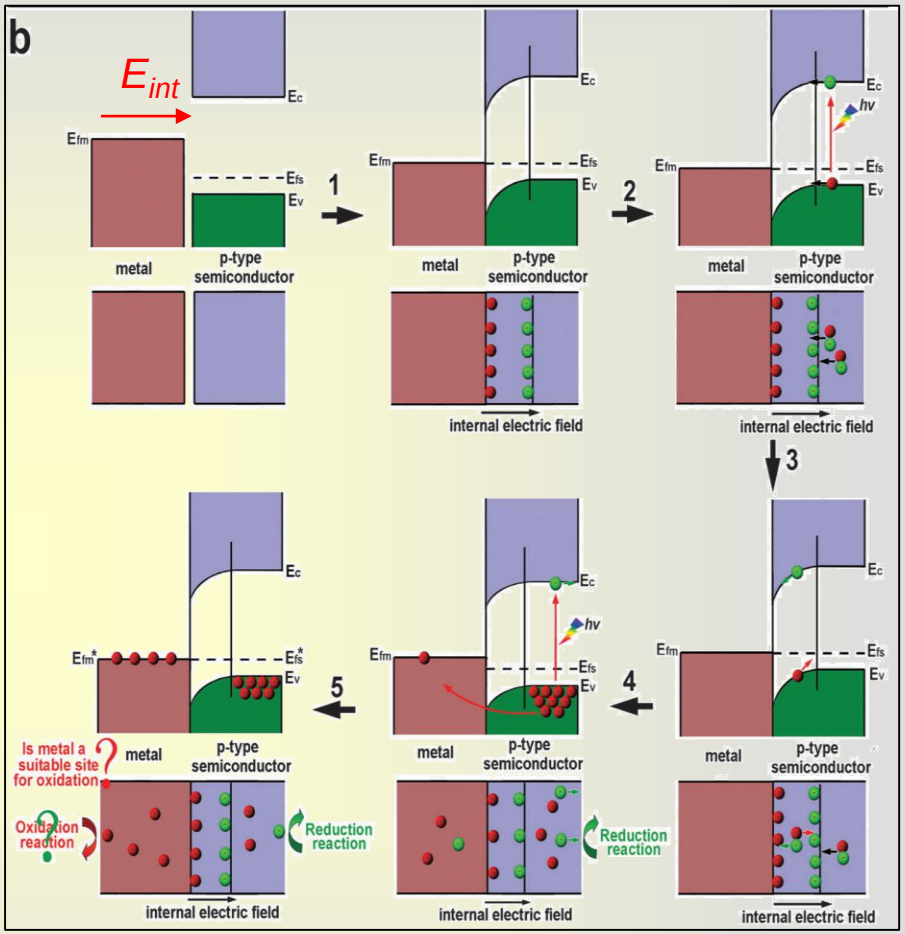

(b) Schematic illustrating processes of charge separation and transfer driven by the Schottky junction between a metal and a p-type semiconductor.

Chem. Soc. Rev. **2015,** *44*, 2893-2939.

Examples of Varied Types of Heterojunctions

Type I (Straddling Alignment) Heterojunctions

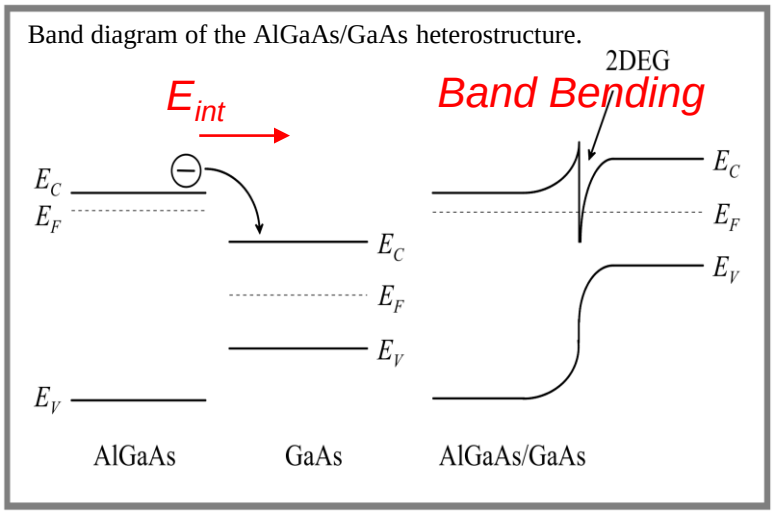

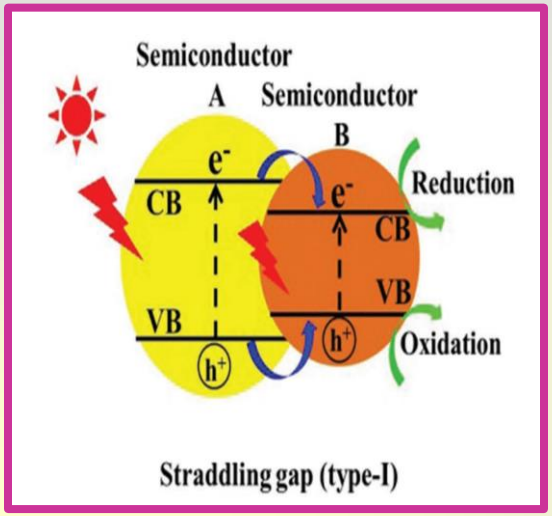

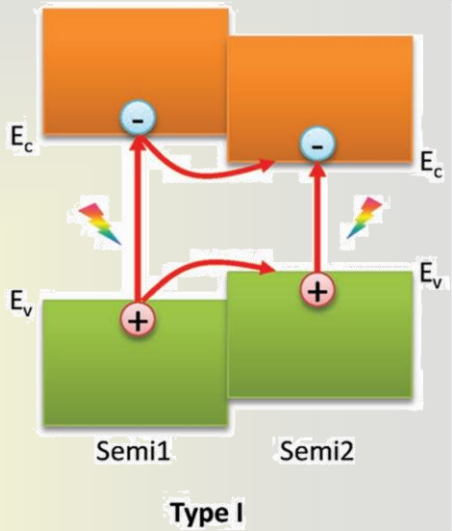

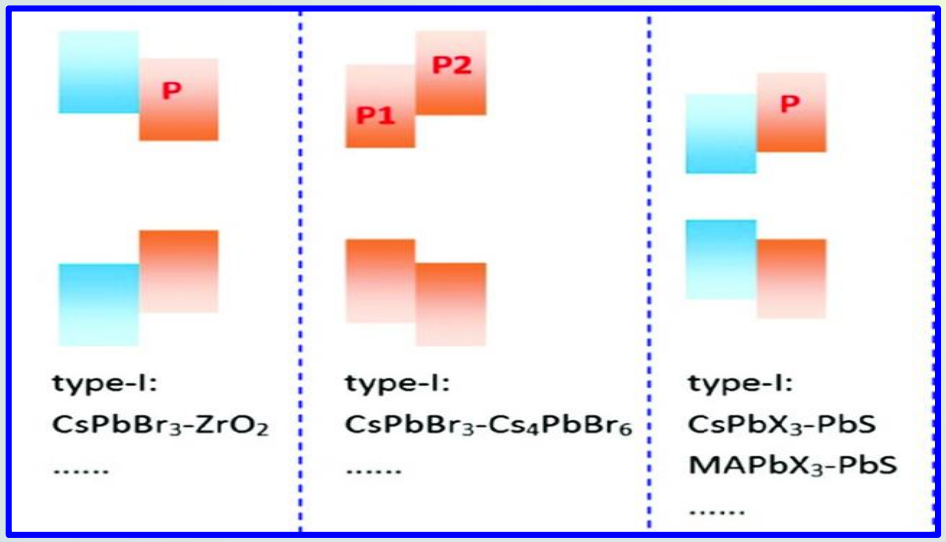

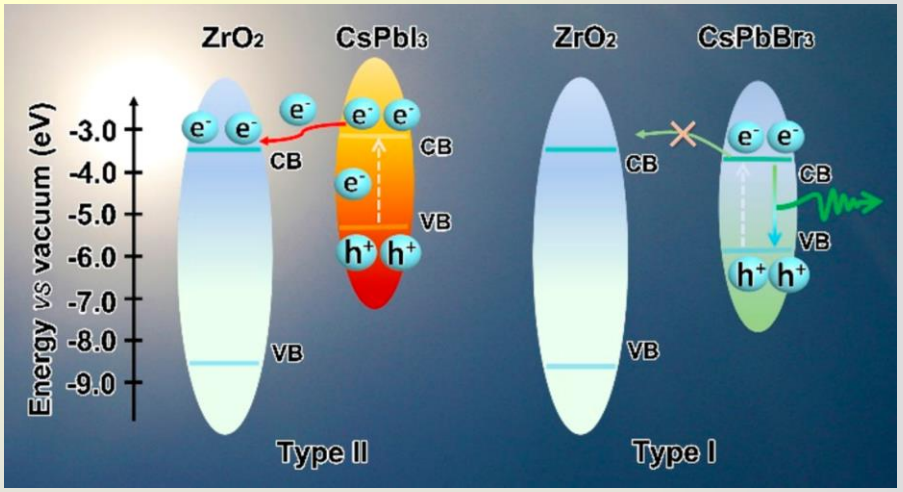

- Small Struct. 1(1), 2020, 2000009
- ACS Nano, 13, 2019, 5366−5374

Type II (Staggered Alignment) Heterojunctions

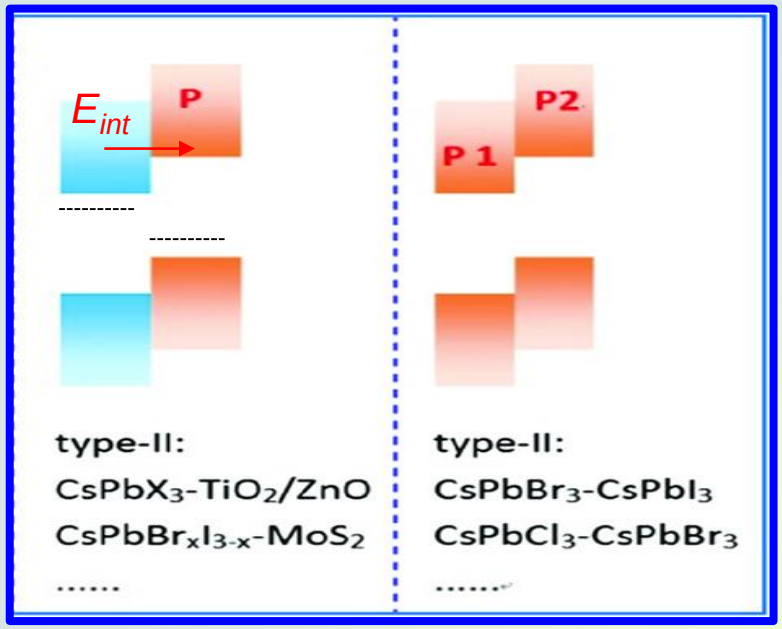

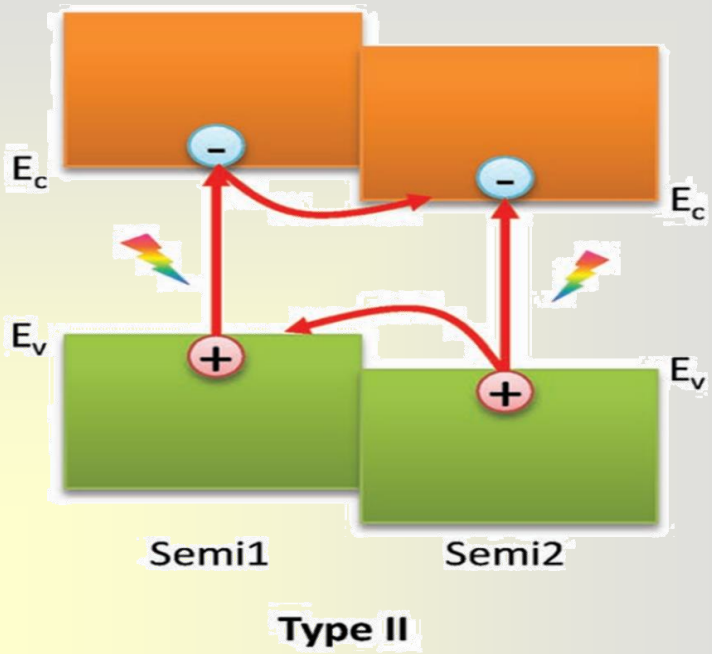

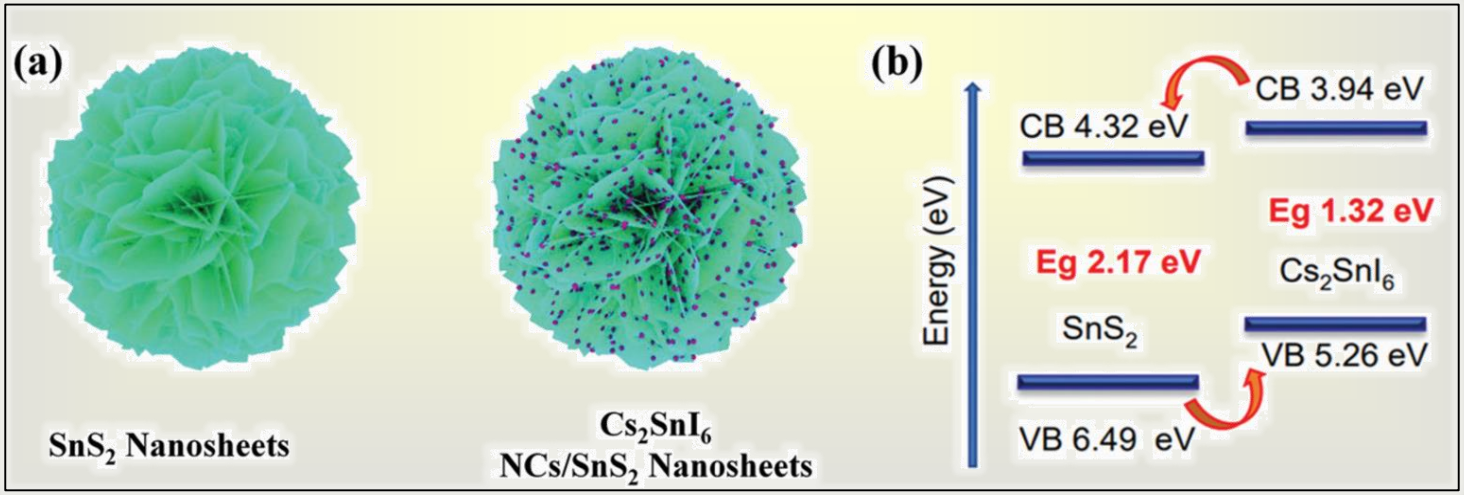

(a) Schematic illustration of the synthesized Cs_2SnI_6/SnS_2 heterostructure. (b) Diagram of the energy band structure of Cs_2SnI_6 and SnS_2.

Small Struct. 1(1), 2020, 2000009. J. Am. Chem. Soc., 2019, 141, 13434–13441.

Type III (broken) Heterojunctions

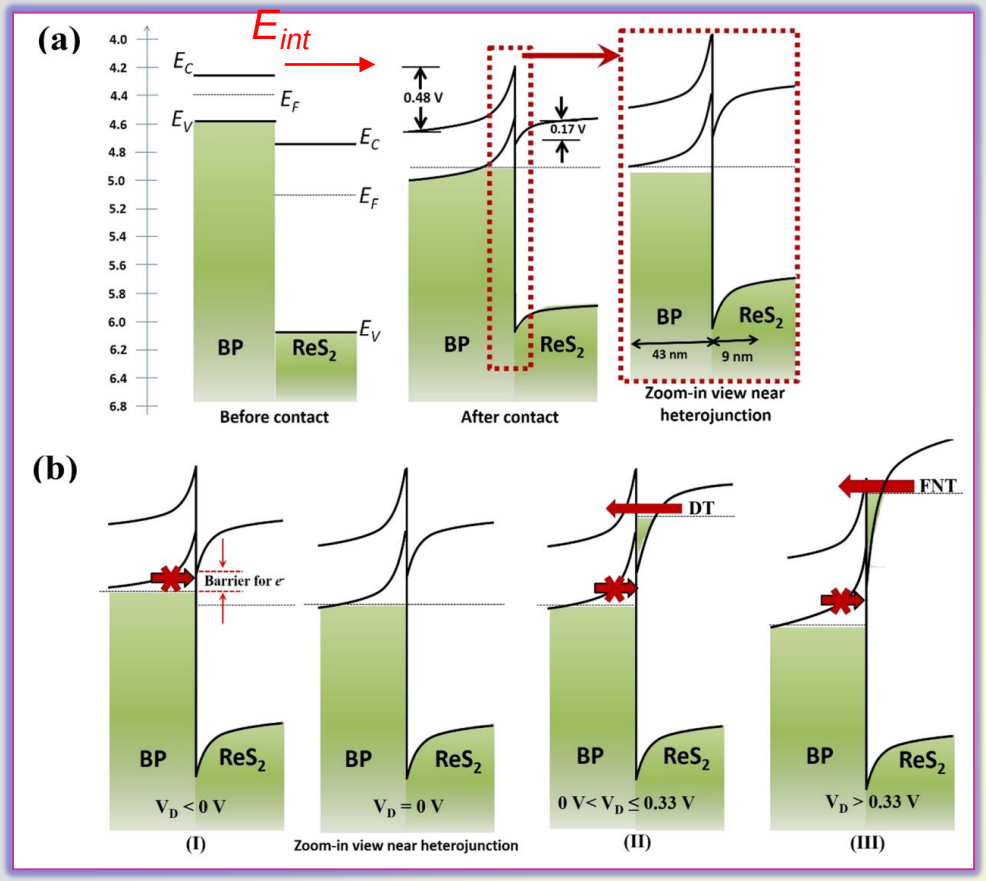

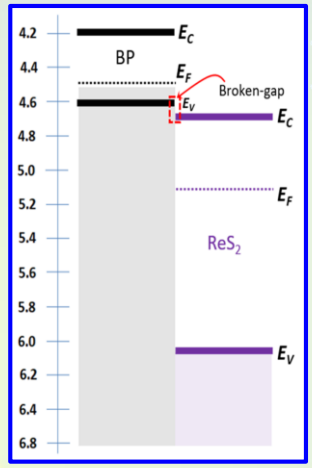

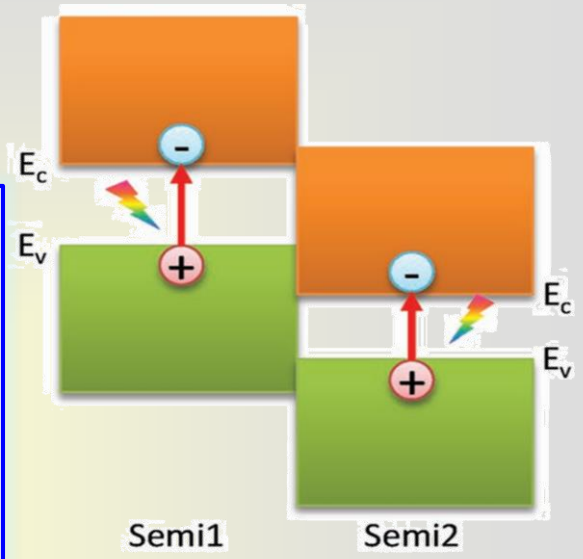

Source | Transistor device | Drain

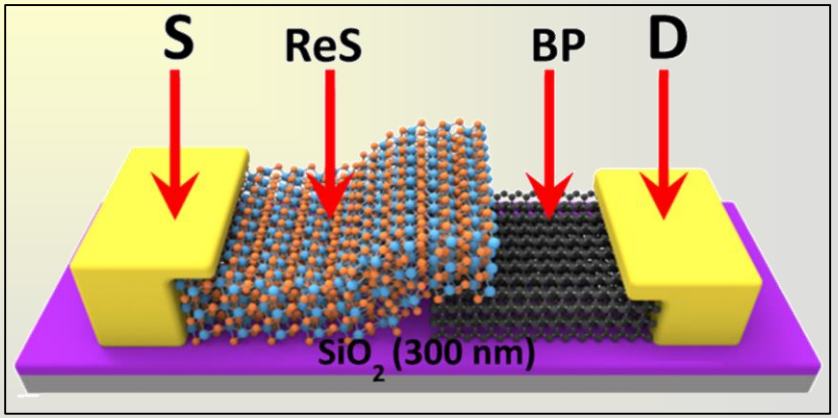

A two-terminal device based on black phosphorus (BP) and rhenium disulfide (ReS_2). Source (S) and drain (D) contacts are labelled.

a) Band alignment at BP/ReS_2 heterojunction before and after equilibrium. Zoom-in view near heterojunction is also shown. Band bending heights in BP and ReS2 regions (V_{bi}(BP) and V_{bi}(ReS_2)) estimated using Poisson's equation are labelled.

b) Effect of drain bias on the band bending near the heterojunction.

BP: black phosphorous

DT: direct tunneling

FNT: Fowler-Nordheim tunneling

ACS Appl. Mater. Interfaces, 11, 2019, 8266−8275.

p-n Junctions

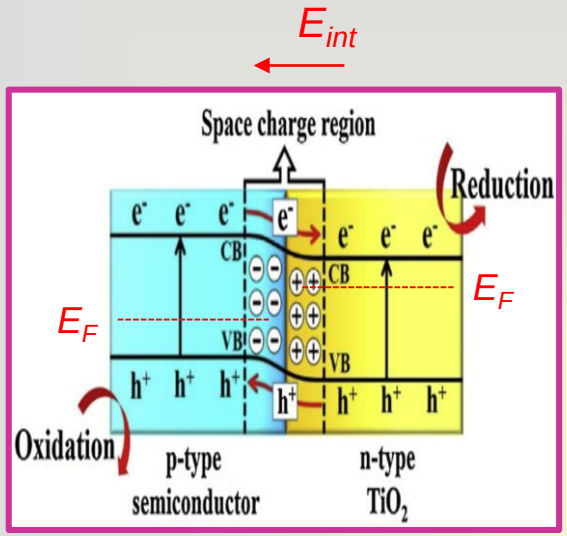

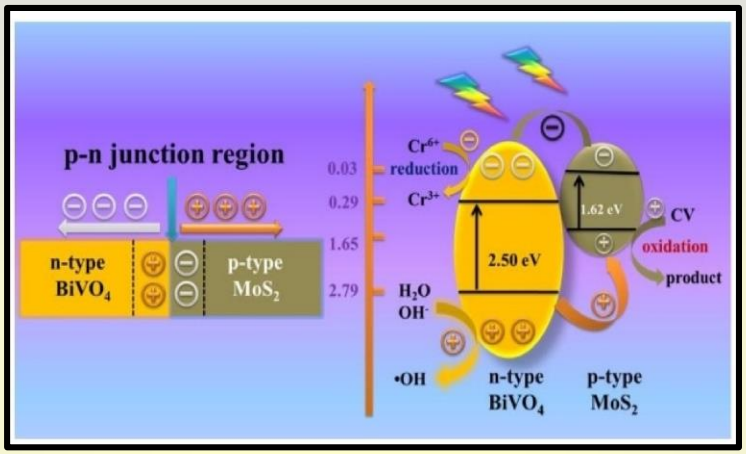

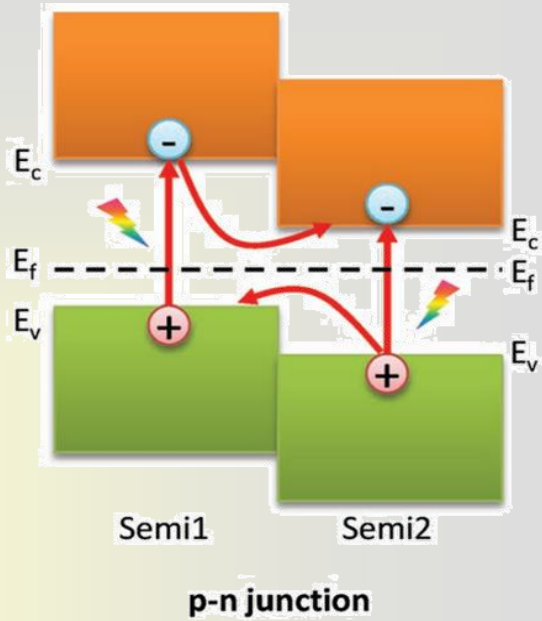

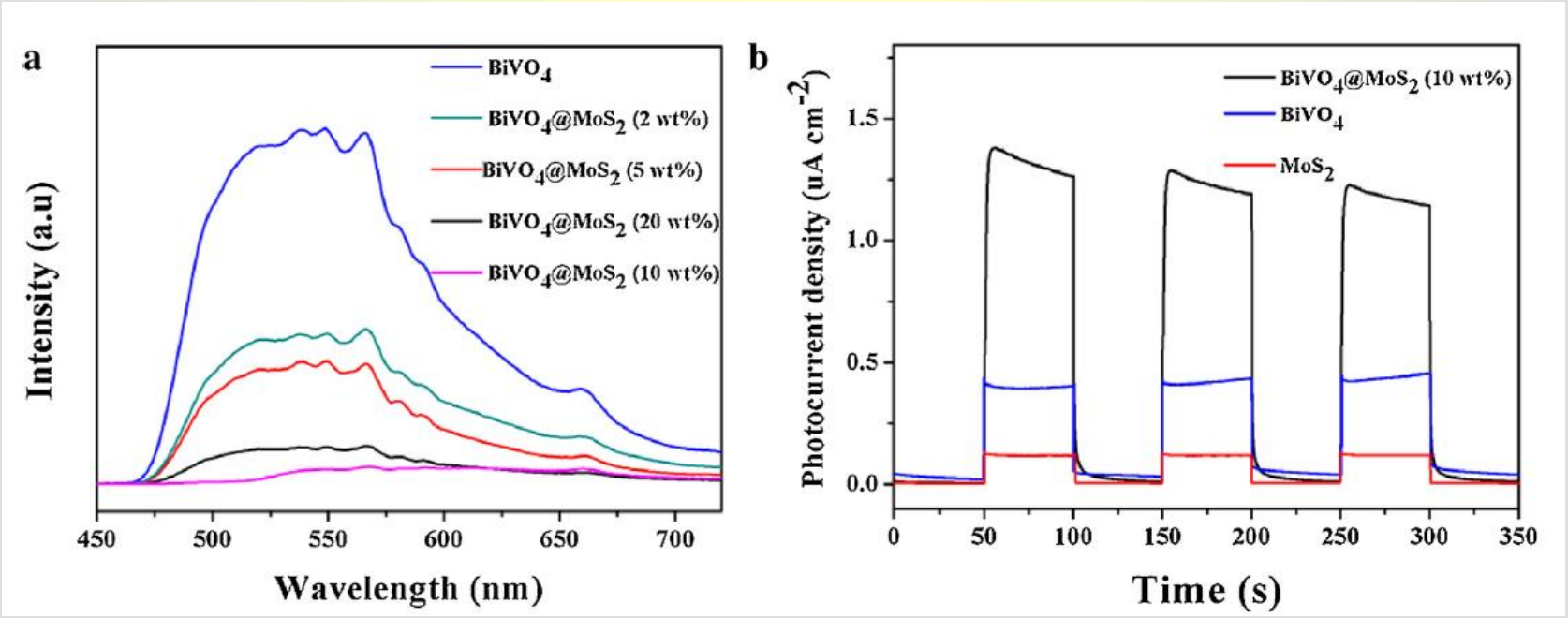

- Applied Catalysis B Environmental, 185, 2016, 242–252.

Traditional Z- Scheme Photocatalytic System

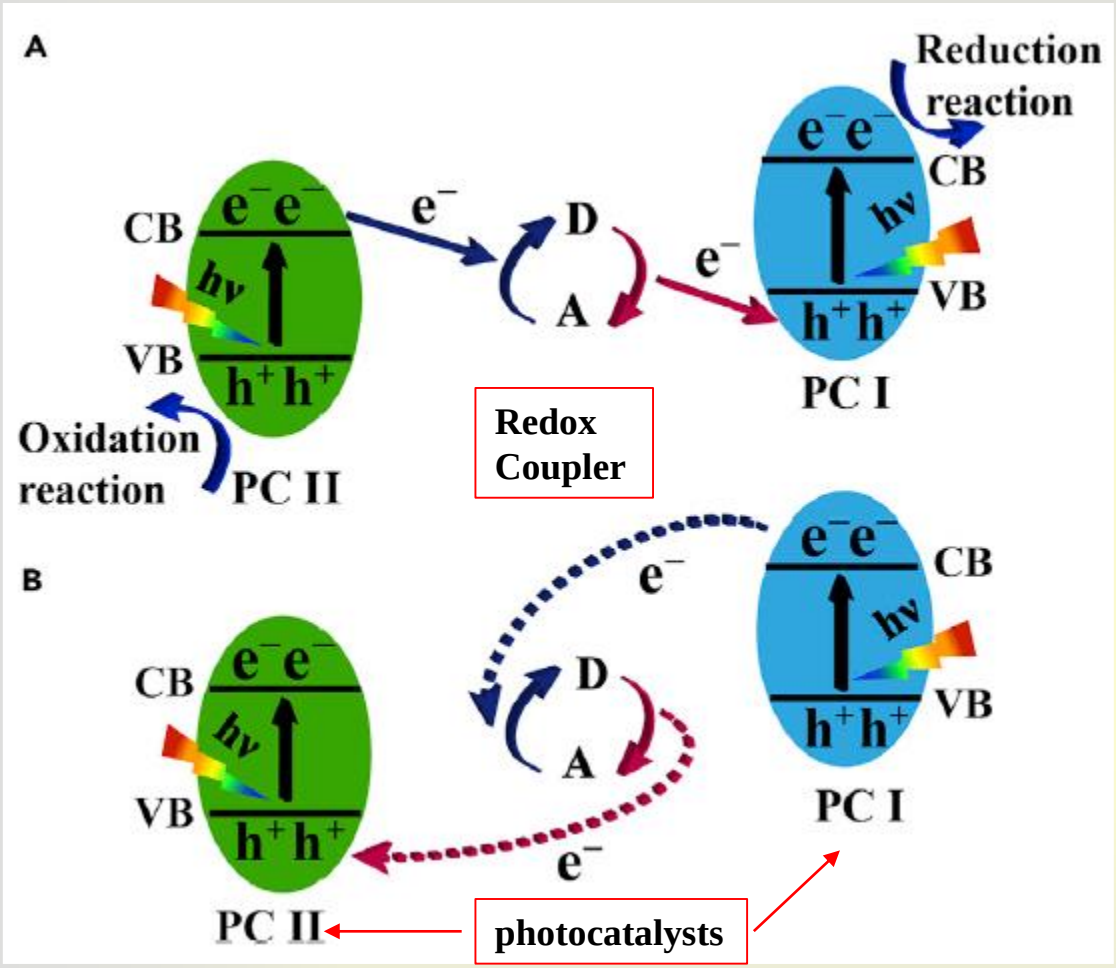

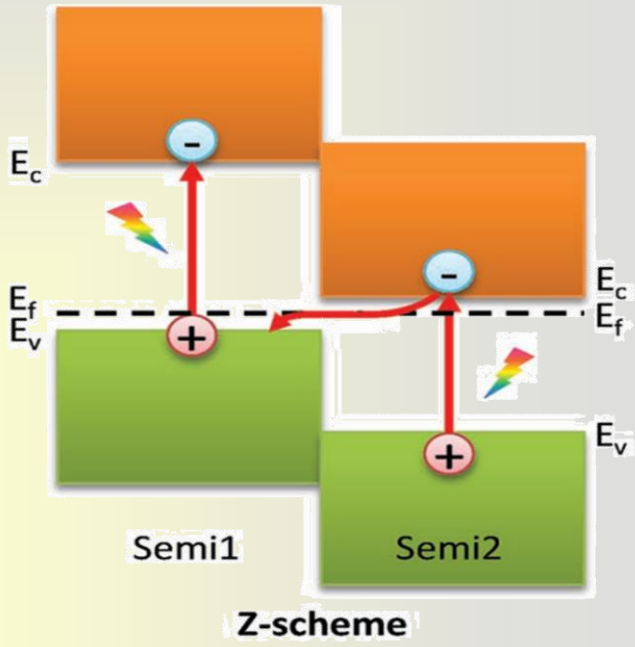

Schematic illustration of the electron–hole separation on the conventional Z-scheme photocatalytic system under light irradiation.

The conventional Z-scheme photocatalysts need a D/A redox coupler that can only be constructed in the liquid phase.

Chem **2020**, *6*, 1543-1559

All Solid-state Z-Scheme Heterojunction

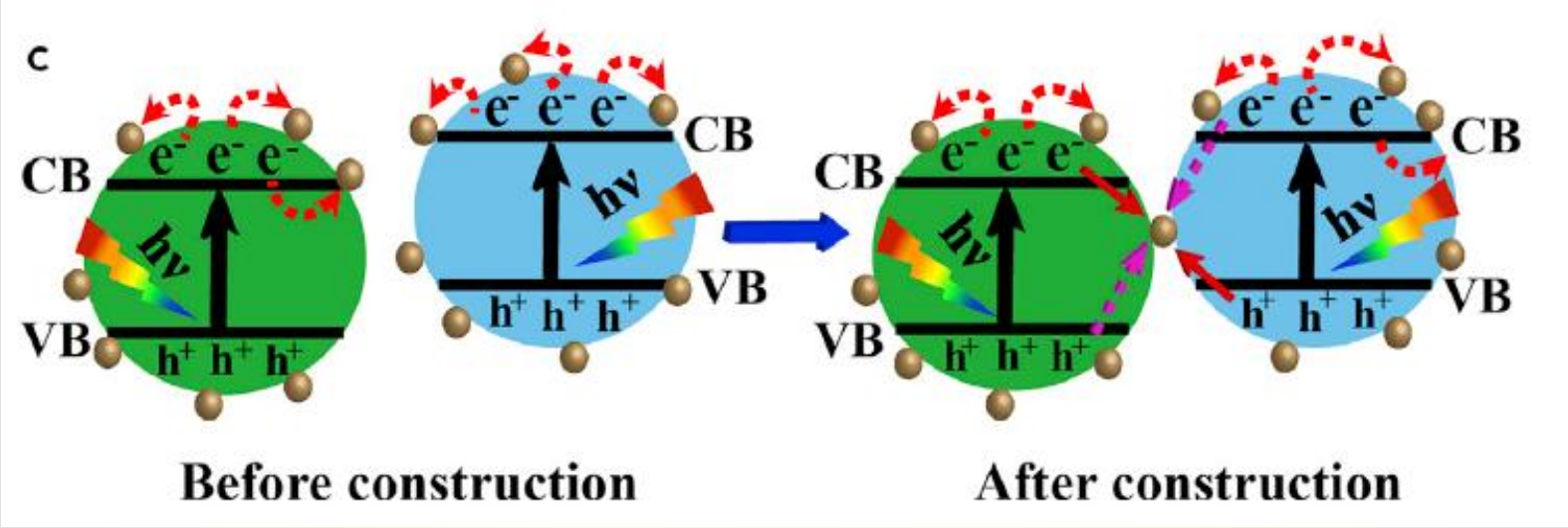

Schematic illustration of all solid-state Z-scheme photocatalysts with an electron mediator under light irradiation.

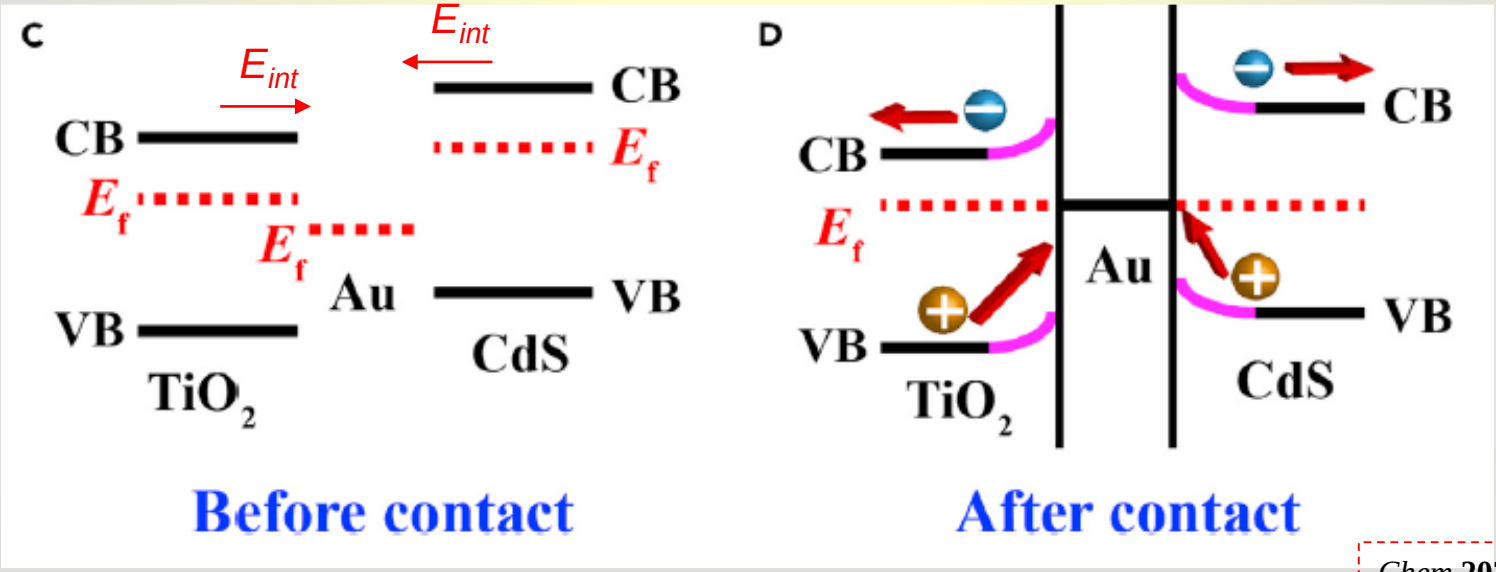

Chem **2020**, *6*, 1543-1559

A Direct Z-Scheme Heterojunction

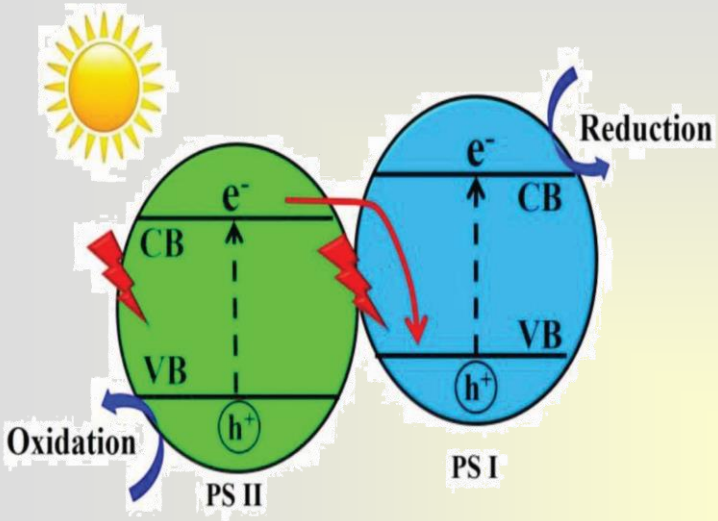

Schematic illustration of the electron–hole separation on a direct Z-scheme photocatalyst under light irradiation.

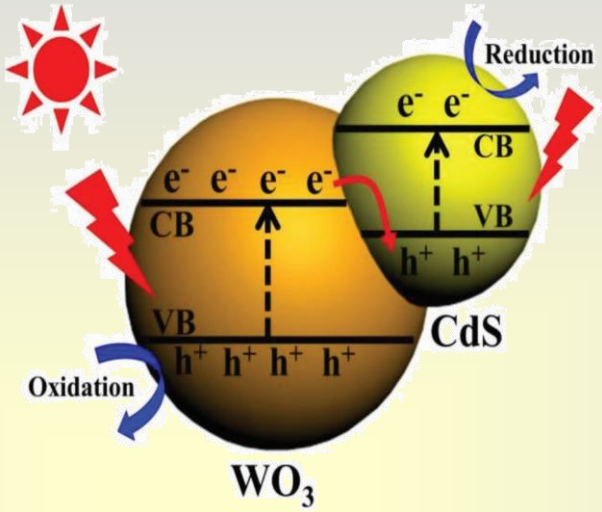

Charge-transfer pathway of the photogenerated electron–hole pairs on CdS–WO_3 direct Z-scheme heterojunction photocatalyst under visible-light irradiation.

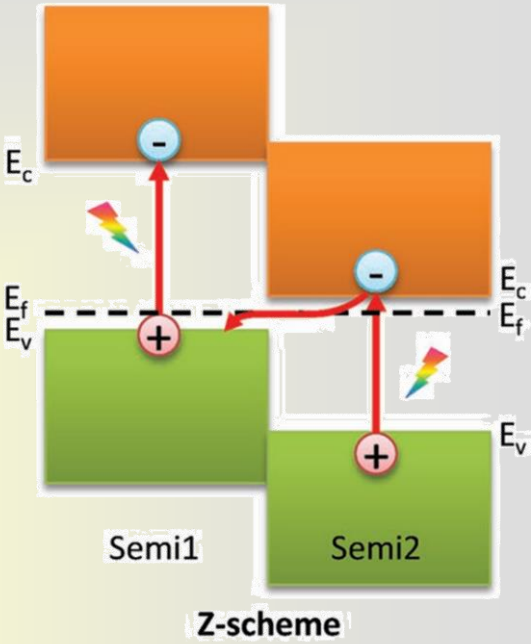

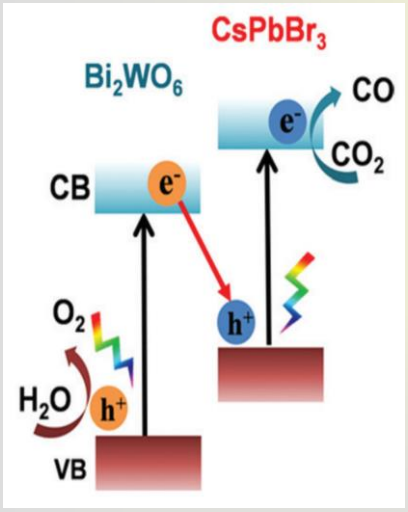

Schematic illustration of Z-scheme of the energy band structure of the $CsPbBr_3/Bi_2WO_6$ composite.

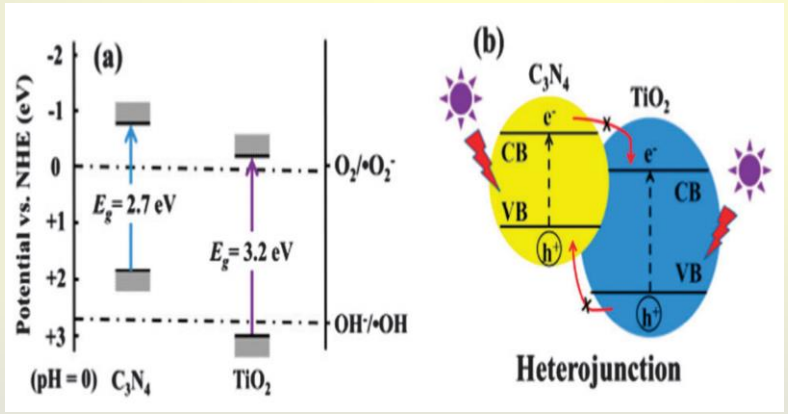

a) Scheme illustrating band positions of g-C_3N_4 and TiO_2 together with redox potentials. b) Conventional g-C_3N_4–TiO_2 heterojunctions cannot form.

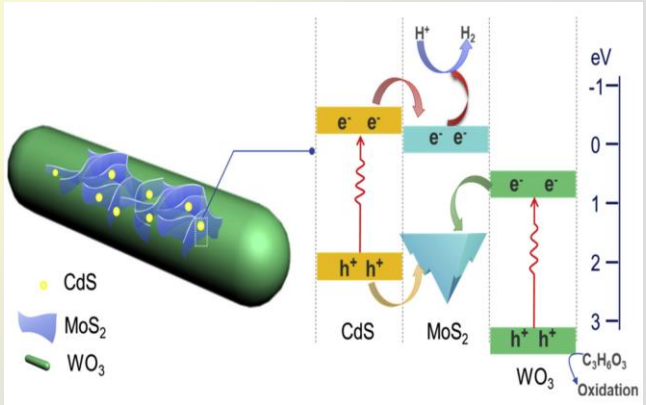

Hybrid Type-II and Z-scheme system

- Adv. Mater., 29, 2017, 1601694.
- Phys. Chem. Chem. Phys., 15, 2013, 16883-16890.
- Applied Catalysis B: Environmental, 259, 2019, 118073.

Schottky Junction vs Z-scheme Heterojunction

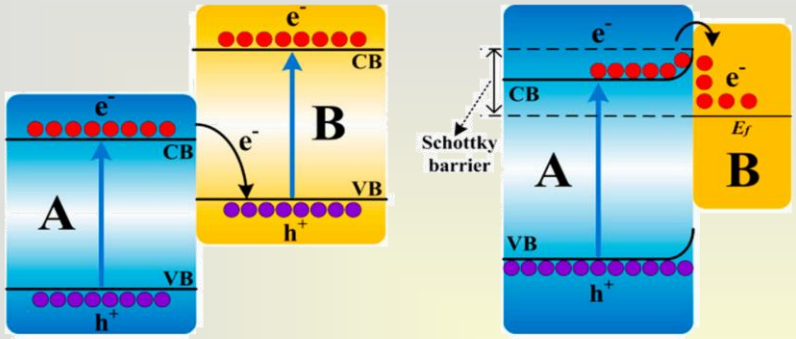

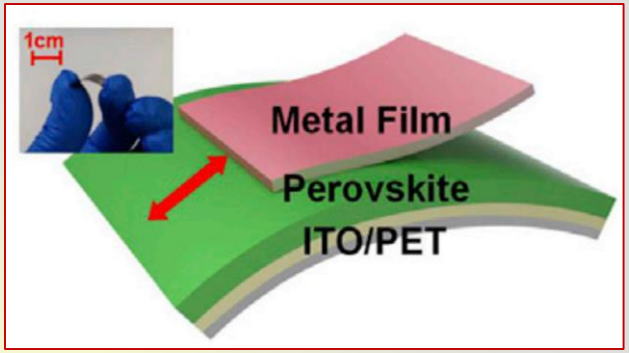

The generator based on a Al/perovskite Schottky junction.

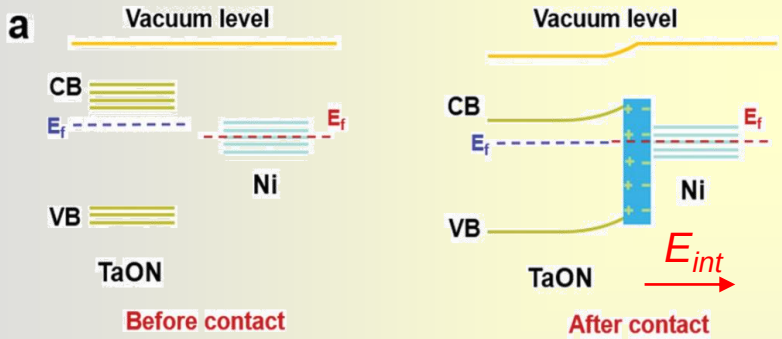

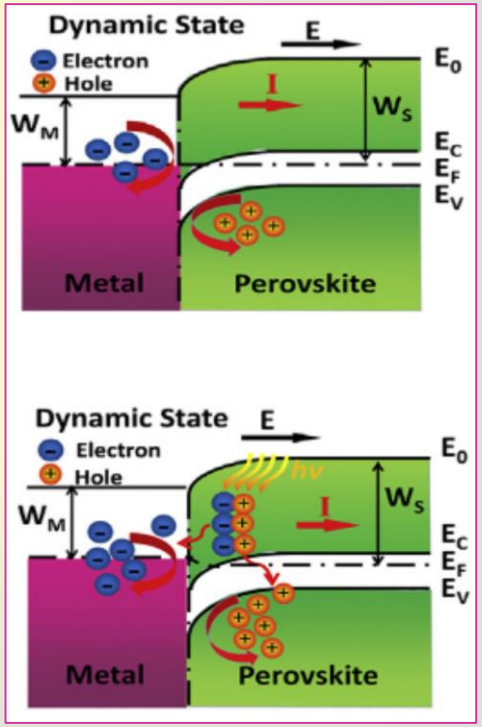

Band structure of the generator based on a dynamic Al/perovskite Schottky junction under dark/light illumination.

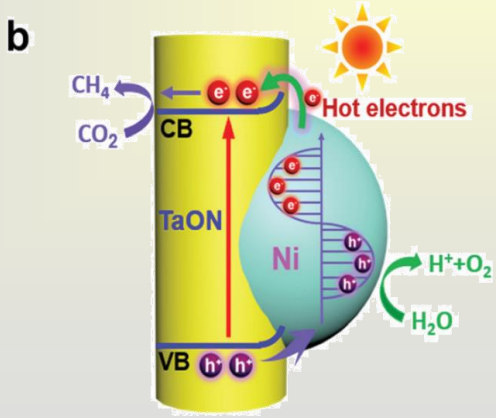

The energy band levels and electrons transfer in TaON@Ni heterostructures.

- Chem. Commun., 55, 2019, 11754.
- Matter 1, 2019, 639–649.

Summary of Varied Types of Heterojunctions

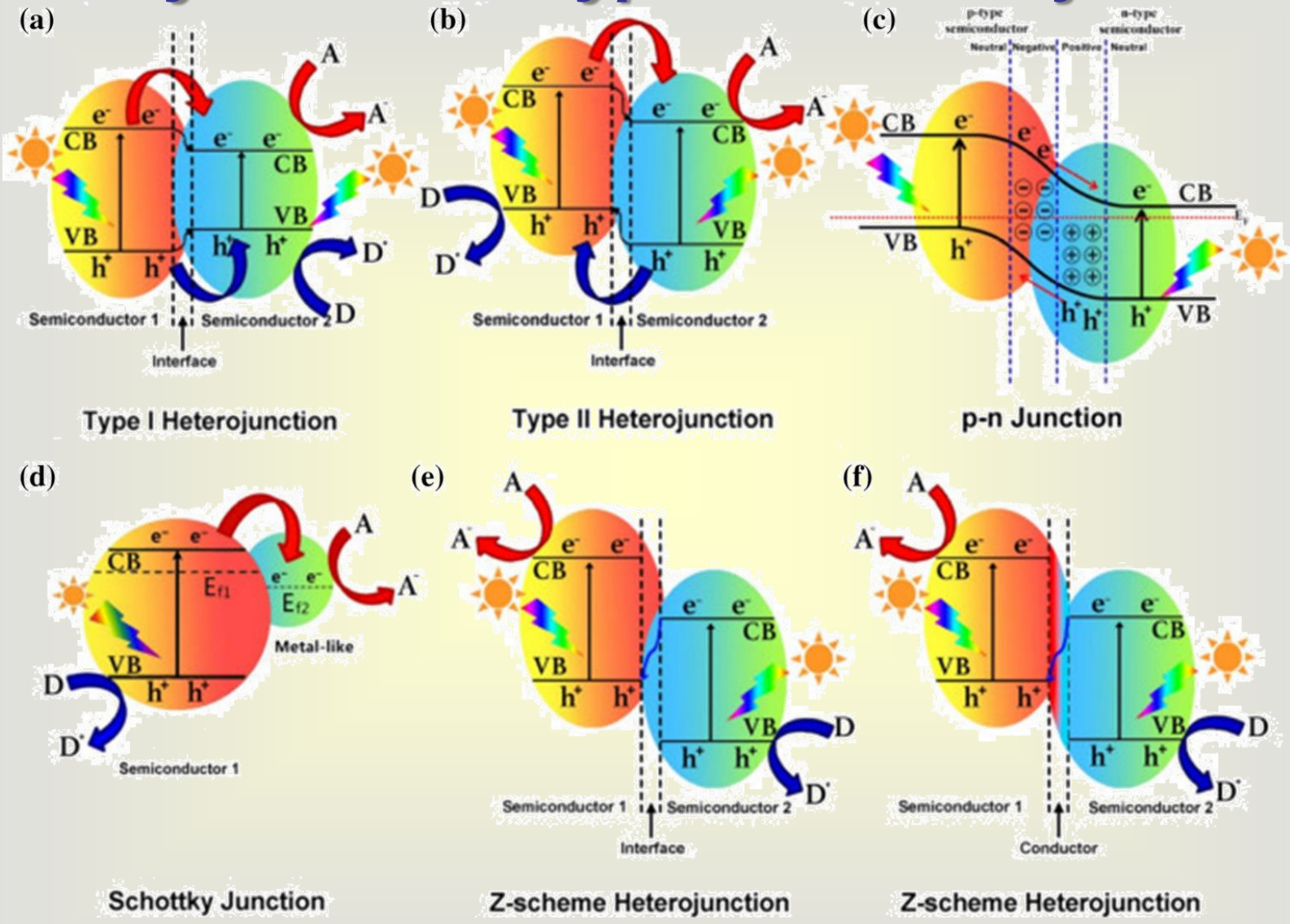

Different types of heterojunctions: a) Type I heterojunction, b) Type II heterojunction, c) p–n junction, d) Schottky junction, e) Z-scheme heterojunction (without an electron mediator), and f) indirect Z-scheme (with an electronmediator).

J. Mater. Sci., 54, 2019, 12206–12235.

A New Type of Heterojunctions: S-Scheme

Step-Scheme (S-Scheme) Photocatalysts

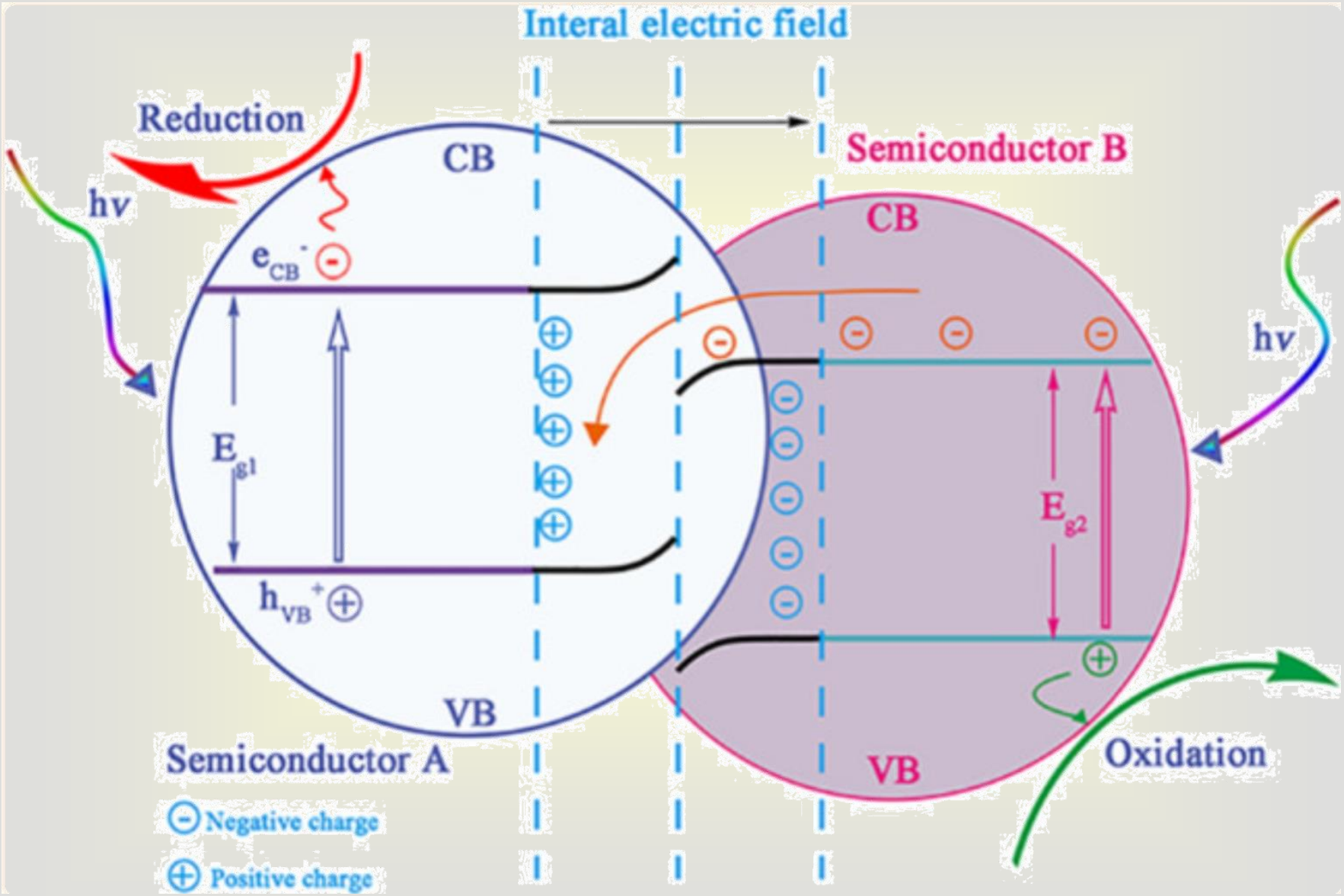

Environ Chem Lett., 6(19), 2021, 4563–4601

S-Scheme Photocatalysts

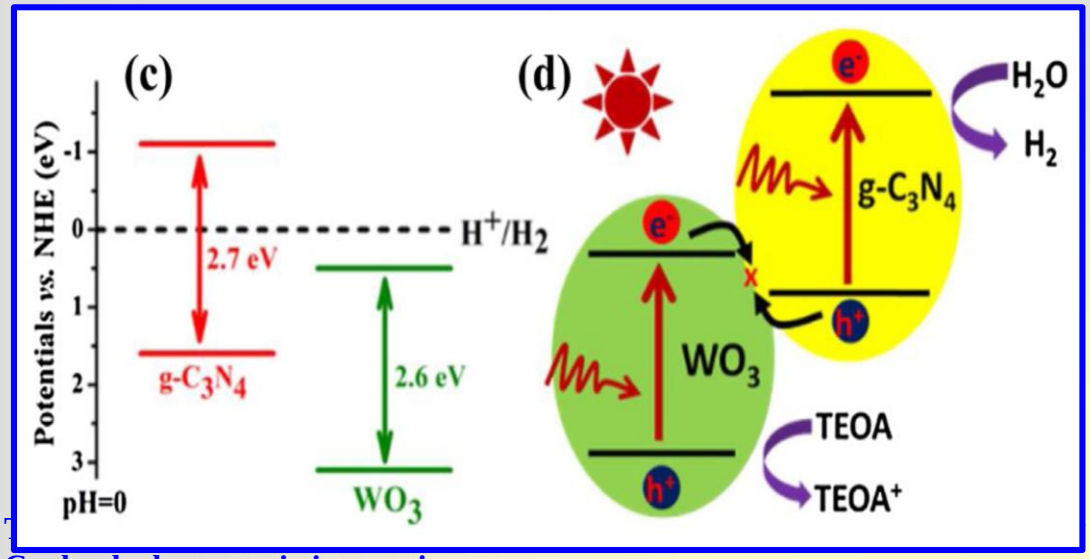

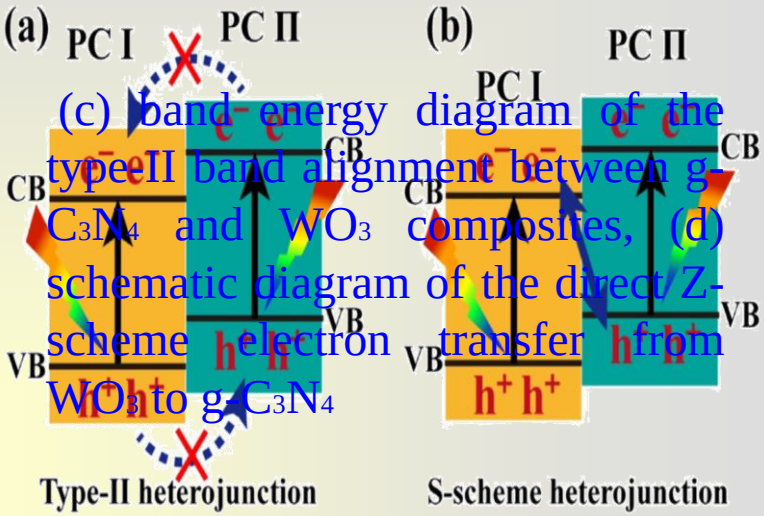

(c) band energy diagram of the type-II band alignment between g-C_3N_4 and WO_3 composites, (d) schematic diagram of the direct Z-scheme electron transfer from WO_3 to g-C_3N_4

Coulomb electrostatic interaction

(a) The work functions of g-C_3N_4 and WO_3 before contact. (b) The internal electric field and band edge bending at the interface of WO_3/g-C_3N_4 after contact. (c) The S-scheme charge transfer mechanism between WO_3 and g-C_3N_4 under light irradiation.

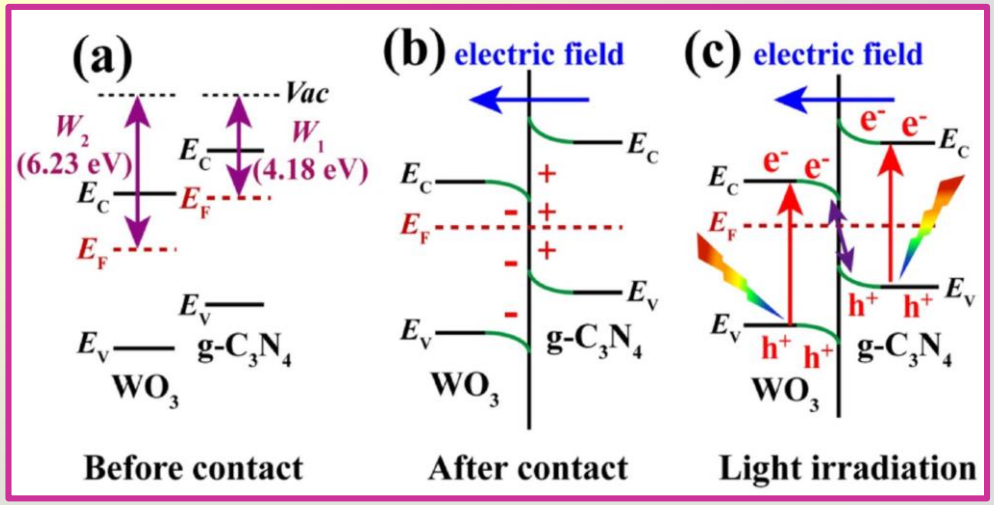

- Applied Catalysis B Environmental 219 (2017) 693–704.
- Applied Catalysis B: Environmental, 243, 2019, 556–565.

Type-II vs S-Scheme Heterojunction

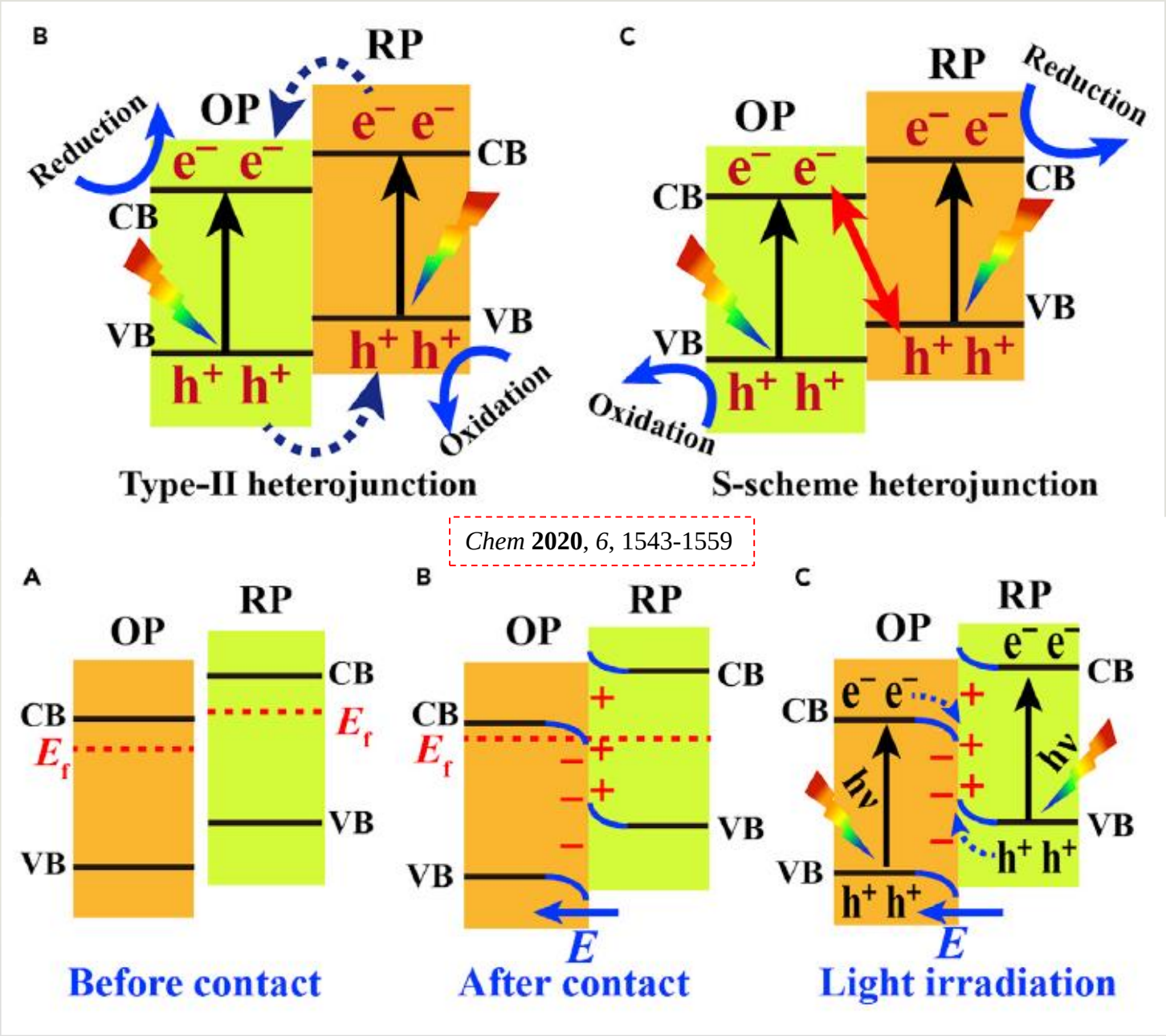

2D-based Heterojunctions for CO_2 Reduction

Graphene Oxide (GO)-based Heterojunctions

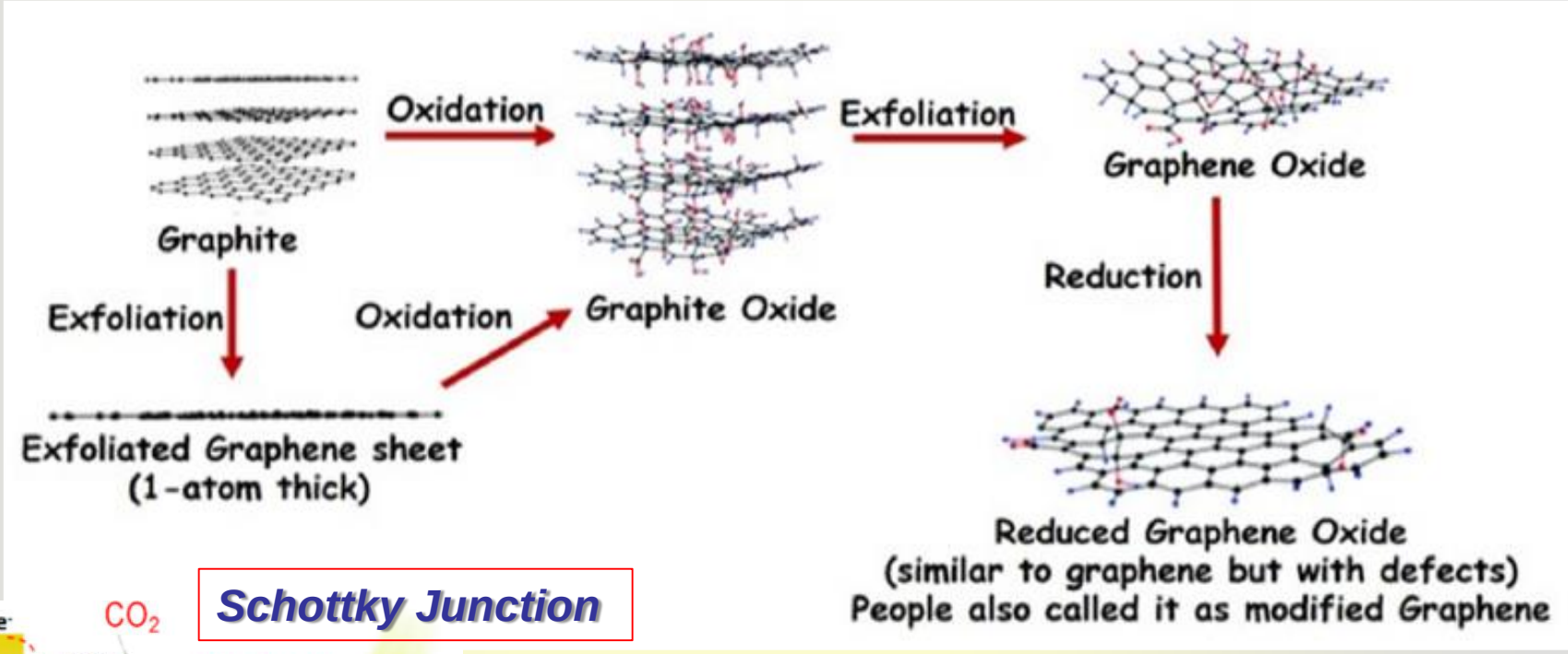

Schottky Junction

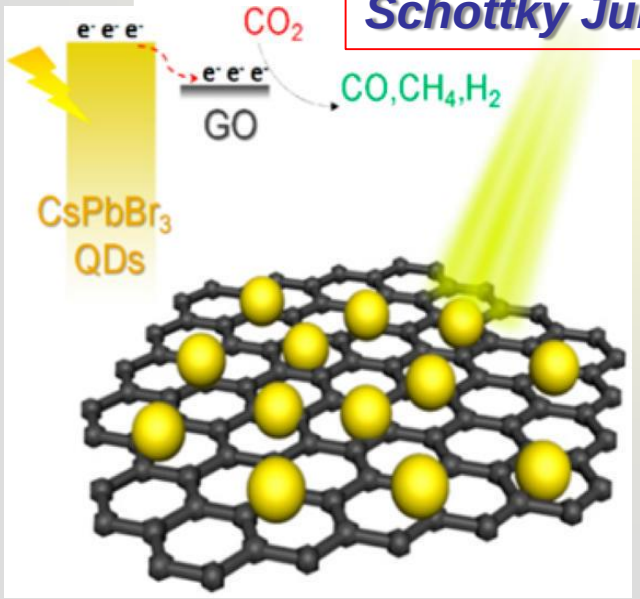

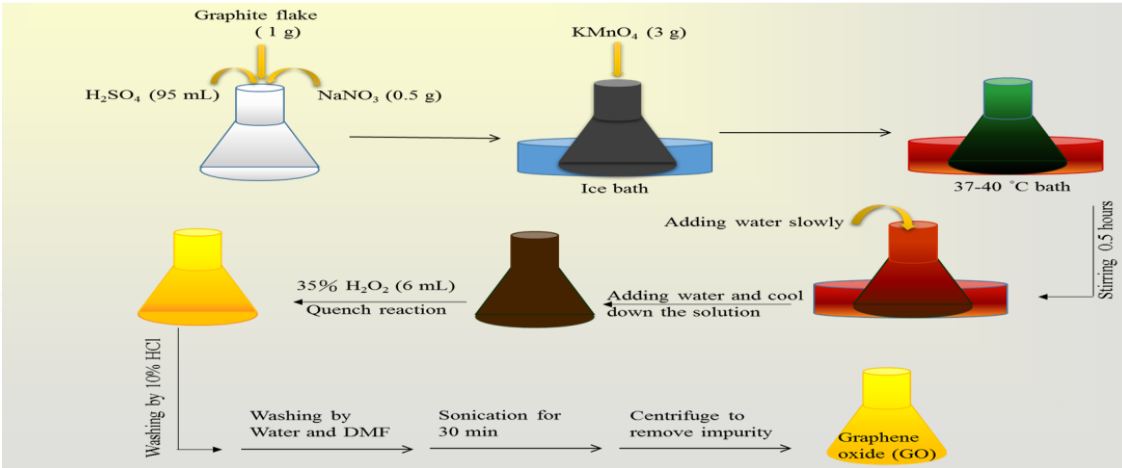

J. Environ. Chem. Engineering **2021**, *9*, 106264.

Graphitic Carbon Nitride (g-C_3N_4)-based Heterojunctions

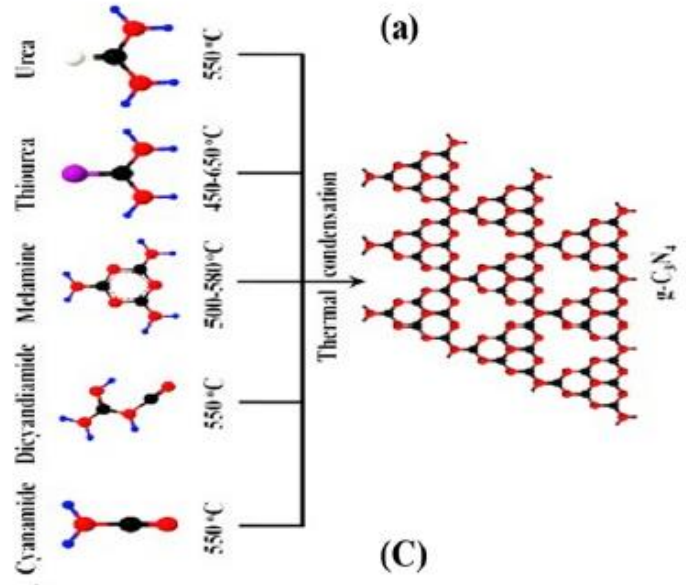

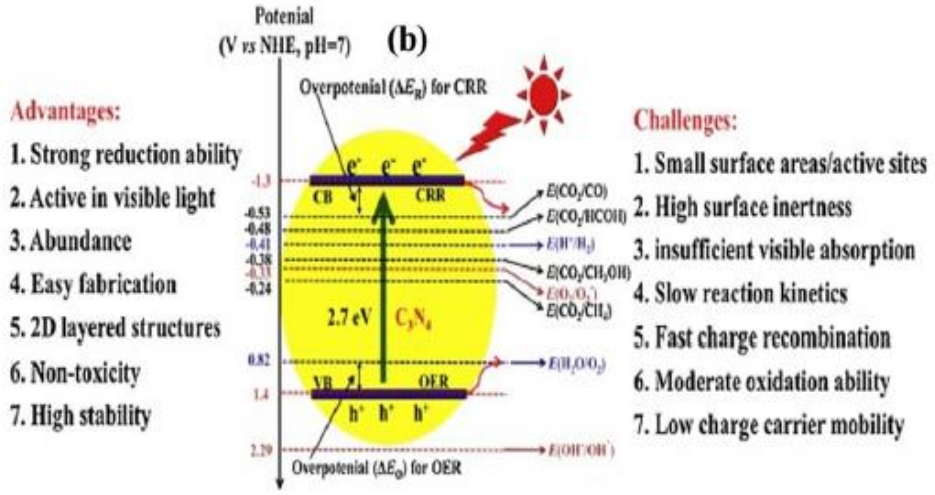

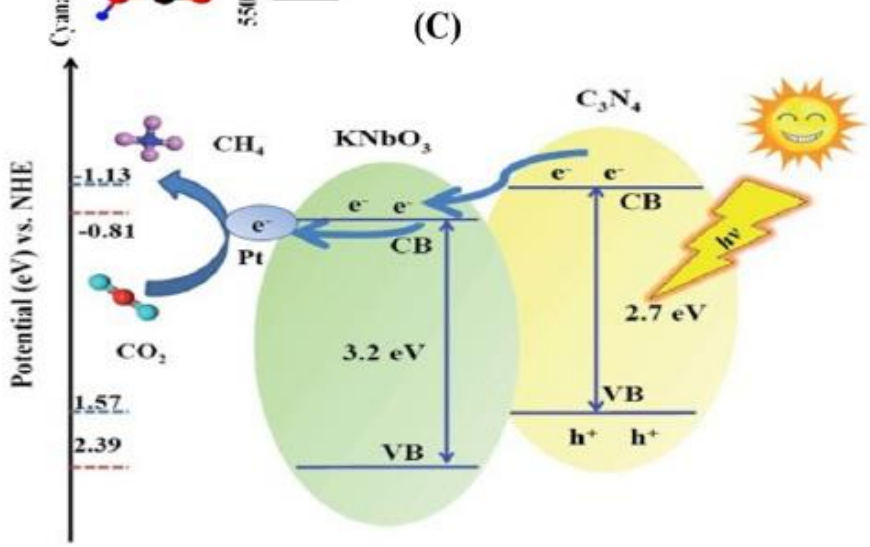

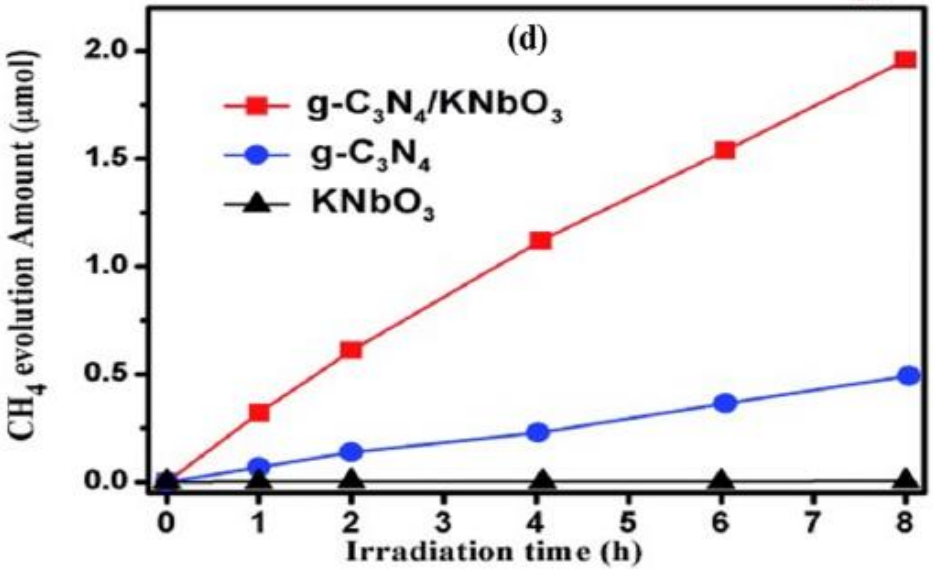

Type-II Heterojunction

J. Environ. Chem. Engineering **2021**, *9*, 106264.

2D Bismuth-based Heterojunctions

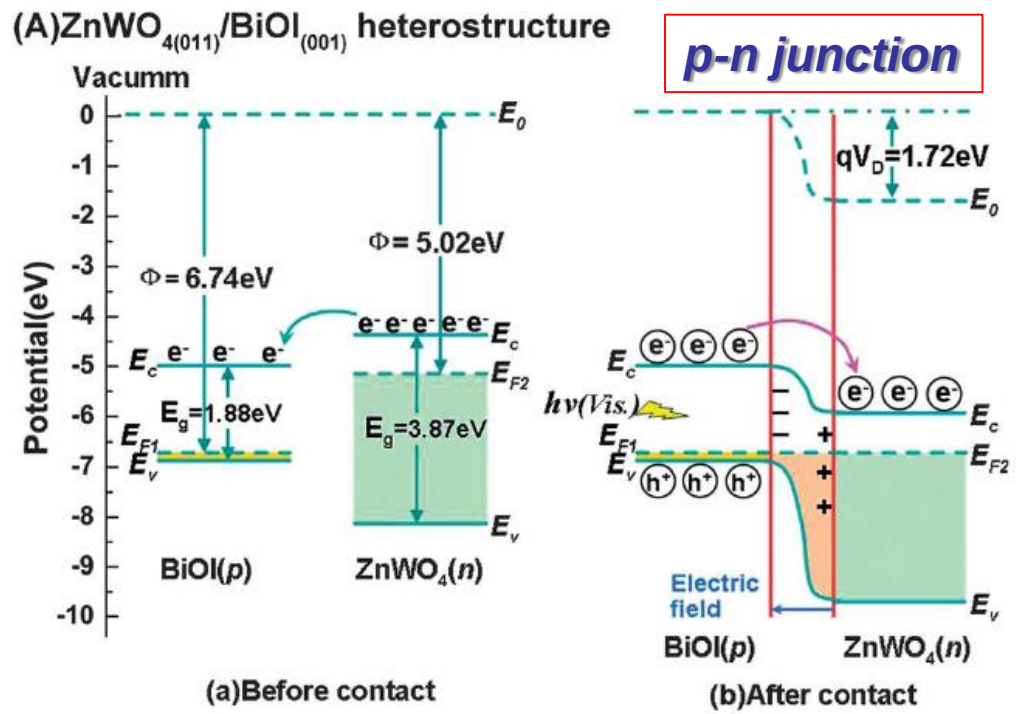

p-n junction

Φ = Work function
E_0 = Vacuum level energy
E_c = Conduction band minimum
E_v = Valence band maximum
E_g = Band gap energy
E_F = Fermi level energy
v_D = Contact potential

J. Mater. Chem. A **2013**, *1*, 3421-3429.

Angew. Chem. Int. Ed. **2019**, *8*, 10873-10878.

Z-scheme heterojunction

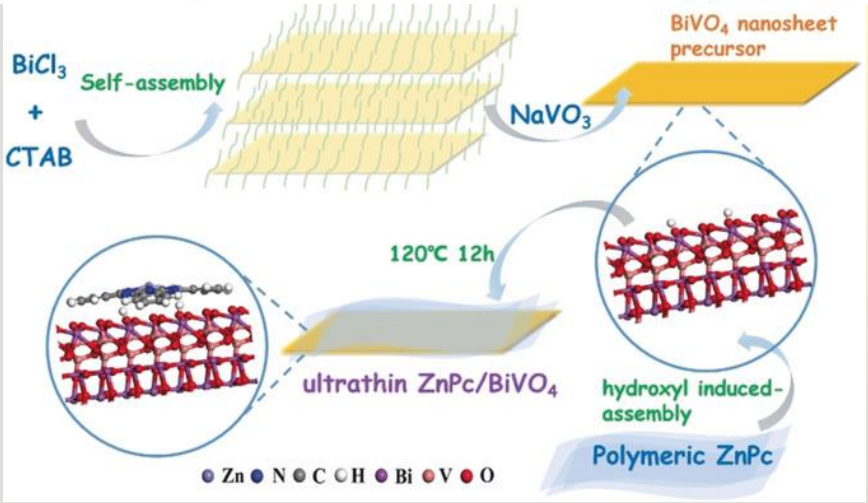

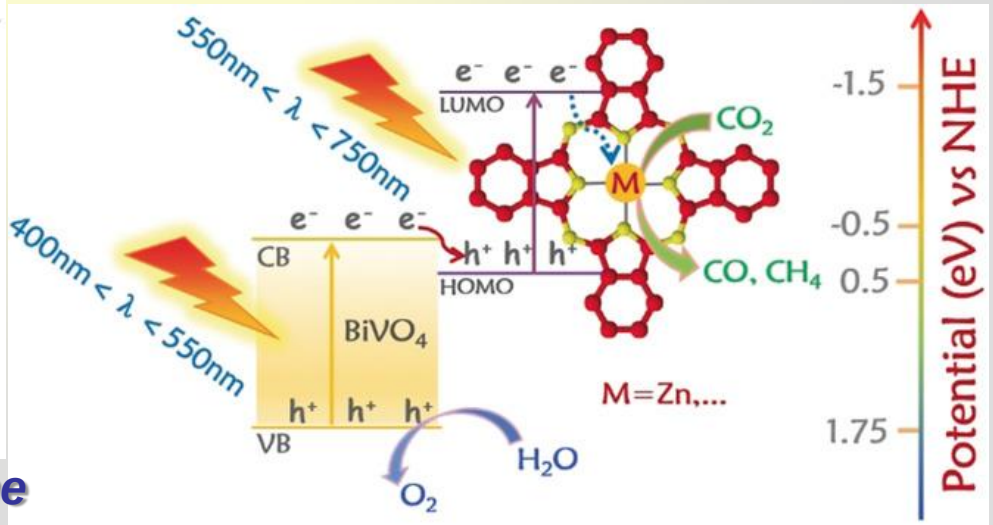

ZnPc = Zinc Pthalocyanine

2D Transition Metal Carbides/Nitrides (MXene)

MAX phases: 211, 312, 413

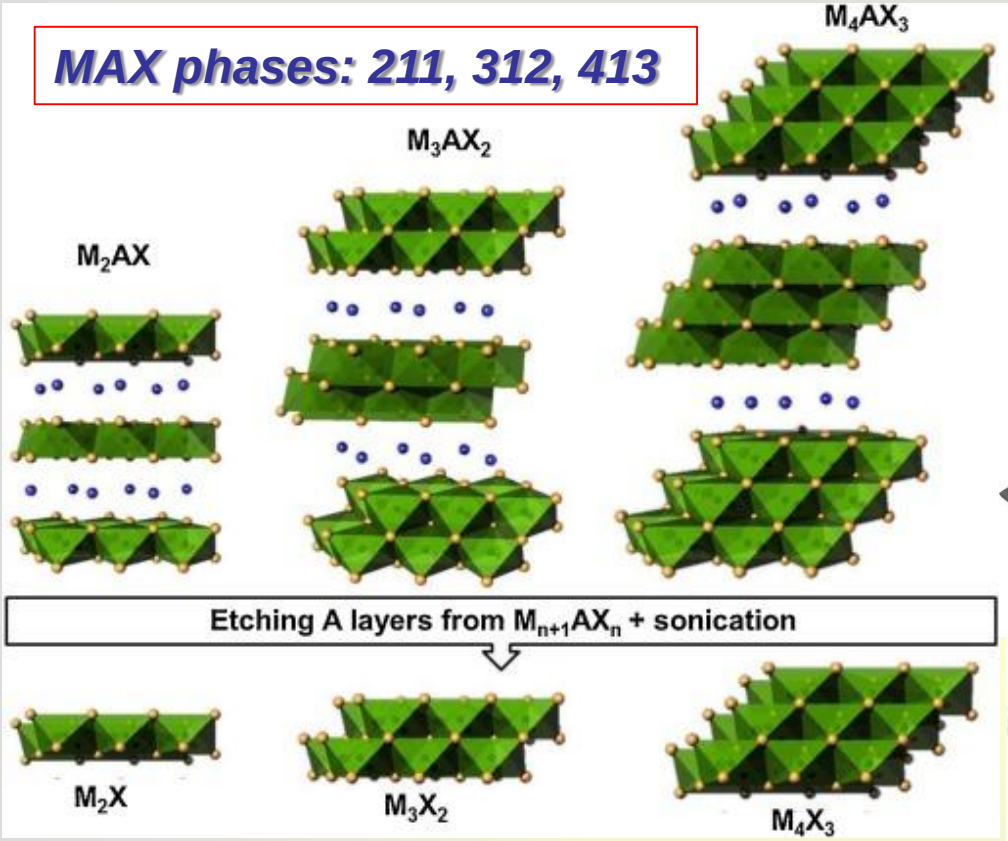

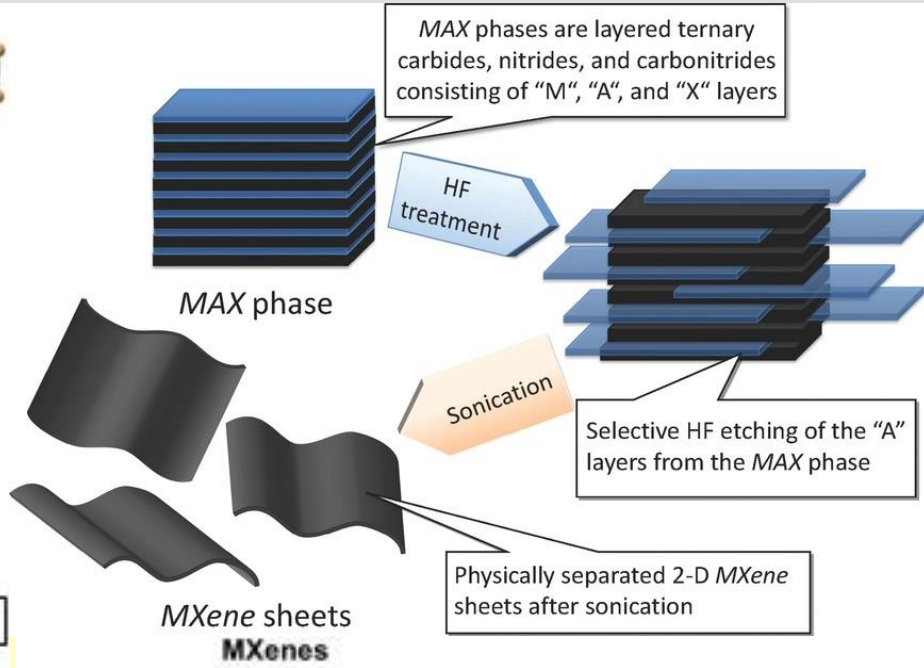

$MXene = M_{n+1}X_n$ (n =1, 2, 3)
M = Sc, Ti, V, Zr, Hf, Nb, Ta, Mo …
X = C and/or N
A = Al, Ga, or Si

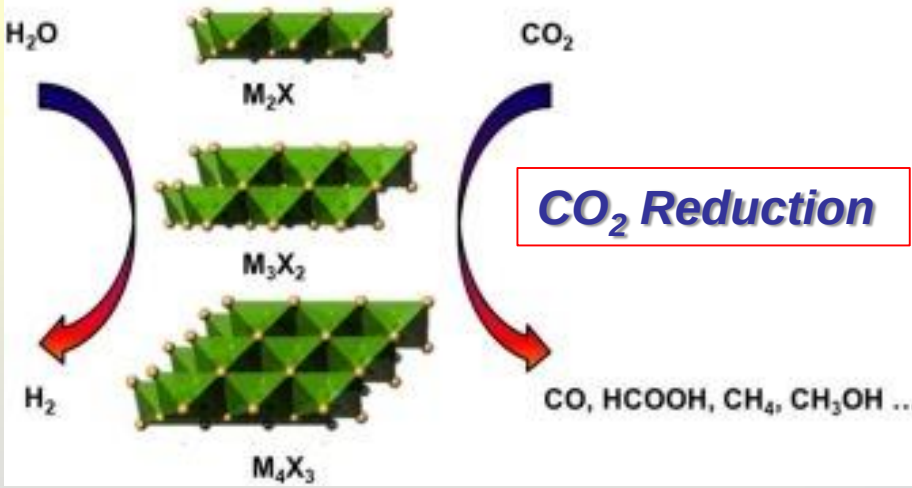

CO_2 Reduction

J. Environ. Chem. Engineering **2021**, *9*, 106264.

Adv. Mater. **2014**, *26*, 992-1005.

MXene-based Heterojunctions

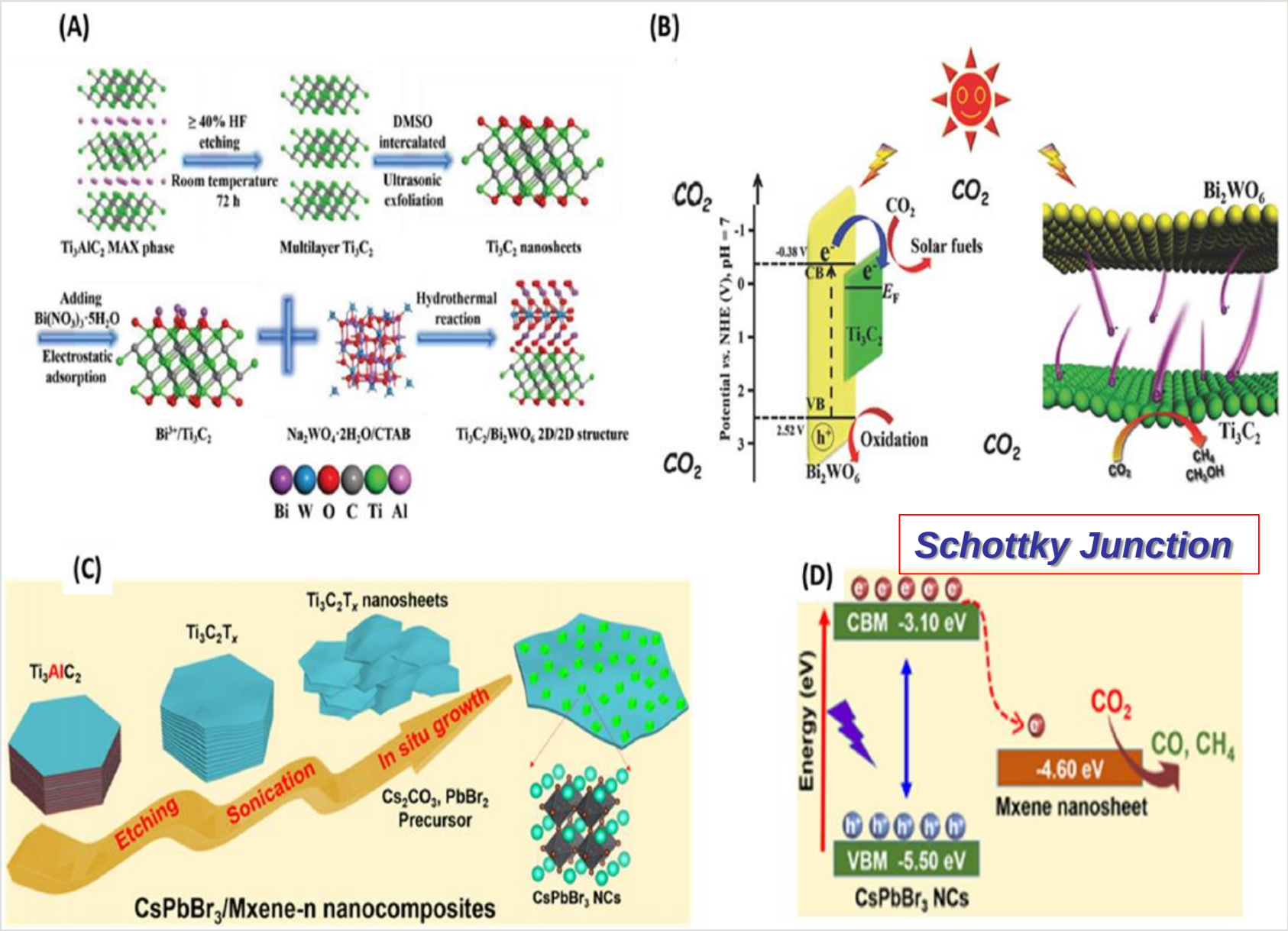

J. Environ. Chem. Engineering **2021**, *9*, 106264.


(C)fuul
Thanks